Journal of Medicinal Chemistry

pubs.acs.org/jmc Article

General Strategy for Integrated Bioorthogonal Prodrugs: Pt(II)-Triggered Depropargylation Enables Controllable Drug Activation *In Vivo*

Tao Sun,[†] Tian Lv,[†] Jianbing Wu,[†] Mingchao Zhu, Yue Fei, Jie Zhu, Yihua Zhang, and Zhangjian Huang*

Cite This: https://dx.doi.org/10.1021/acs.jmedchem.0c01435 Read Online

ACCESS | Metrics & More | Article Recommendations | Supporting Information

ABSTRACT: Bioorthogonal decaging reactions for controllable drug activation within complex biological systems are highly desirable yet extremely challenging. Herein, we find a new class of Pt(II)-triggered bioorthogonal cleavage reactions in which Pt(II) but not Pt(IV) complexes effectively trigger the cleavage of *O*/*N*-propargyl in a variety of ranges of caged molecules under biocompatible conditions. Based on these findings, we propose a general strategy for integrated bioorthogonal prodrugs and accordingly design a prodrug **16**, in which a Pt(IV) moiety is covalently connected with an O^2-propargyl diazeniumdiolate moiety. It is found that **16** can be specifically reduced by cytoplasmic reductants in human ovarian cancer cells to liberate cisplatin, which subsequently stimulates the cleavage of O^2-propargyl to release large amounts of NO *in situ*, thus generating synergistic and potent tumor suppression activity *in vivo*. Therefore, Pt(II)-triggered depropargylation and the integration concept might provide a general strategy for broad applicability of bioorthogonal cleavage chemistry *in vivo*.

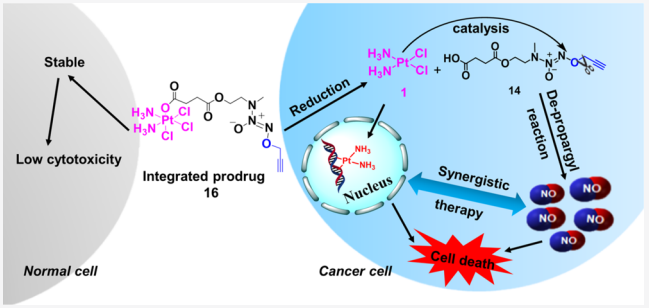

INTRODUCTION

Bioorthogonal chemistry, which is defined as any facile and friendly chemical reaction that can occur inside aqueous living systems,[1−4] has an increasing impact on chemical biology and medicinal chemistry. To date, bioorthogonal chemistry has been extensively utilized to modulate biomolecules of interest via "bond formation" or "bond cleavage" reactions.[5−8] Some bioorthogonal bond cleavage reactions, in which cleavage reagents (B) including transition-metals (Pd, Ru, and Au) and tetrazines mediate uncaging reactions from caged active groups (A−C), have been successfully employed to develop bioorthogonal cleavage reaction-based prodrugs in the arena of cancer therapy (Figure 1A).[9−19] For instance, gold-triggered depropargylation from the prodrugs generated floxuridine or doxorubicin, displaying potent anticancer activity,[10] combination of 5-fluoro-1-propargyl-uracil and Pd(0)-functionalized resins exhibited strong antiproliferative properties,[11] as well as tetrazine-mediated bond cleavage of 3-isocyanopropyl enabled the controlled release of doxorubicin and mitomycin, significantly inhibiting cancer cell growth.[15] Compared with enzyme-activatable prodrugs, bioorthogonal cleavage reaction-based prodrugs rely on extrinsic and biocompatible agents to achieve a superior spatiotemporal drug function, thus minimizing off-targeting activation and consequent adverse effects.[11,20]

Although much progress has been made in the past few years in developing bioorthogonal cleavage reactions for prodrug activation, some challenges still remain. Cleavage reagents (B) and caged active agents (A−C) are usually separated,[7−10] and the reactions between them lack control in terms of location, limiting broad therapeutic applications *in vivo*.[19,21] There are published methods including intratumor injection of cleavage reagents,[22] supramolecular self-assembly of cleavage reagents triggered by enzymes unique in cancer,[23] and exosome loading of ultrathin palladium nanosheets,[24] which allow for enrichment of the cleavage reactions in cancer.

Nevertheless, to the best of our knowledge, direct modification of cleavage reagents to achieve the desired selectivity for cancer cells has not been reported yet. To address the traditional shortcomings of bioorthogonal activation chemistry, we hypothesize that direct modification of cleavage reagents (masked-B) could mask its uncaging ability but selectively recover in a tumor microenvironment (Figure 1B), and further covalent coupling of the modified cleavage reagents (masked-B) with the caged active agents (A−C) would provide

Received: August 25, 2020

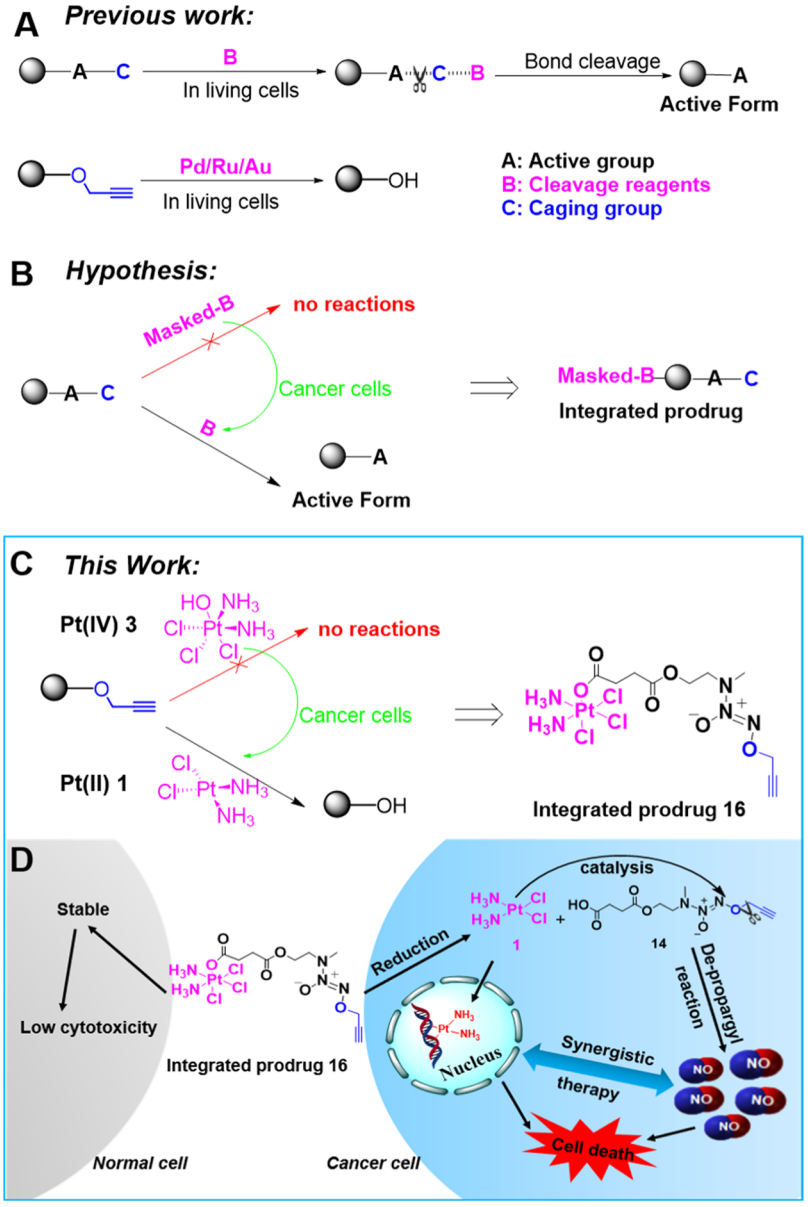

Figure 1. (A) Previous work: cleavage reagent (B) triggers the uncaging process of caged active agents (A−C) to release the active group A. (B) Hypothesis: masked-B could mask the uncaging activity but regenerate the uncaging activity in cancer cells. (C) This work: Pt(II) **1** effectively catalyzes the depropargylation of **5a**, whereas Pt(IV) **3** does not. Based on this finding, an integrated bioorthogonal prodrug **16** is designed and synthesized for proof-of-concept. (D) Proposed mechanism of **16**: as an inert Pt(IV) derivative, **16** could be specifically reduced by cytoplasmic reductants in cancer cells to release **1** and O^2-diazeniumdiolate **14**. Then, **1** triggers the bond cleavage of O^2-propargyl in **14** to liberate large amounts of NO *in situ*, generating selective and synergistic anticancer activity *in vivo*.

a hitherto-unknown class of integrated bioorthogonal cleavage reaction-based prodrug (masked-B-A-C, Figure 1B). It is proposed that masked-B-A-C could be inert, avoiding intermolecular bioorthogonal reactions. After being selectively activated in living cancer cells, masked-B-A-C would liberate the cleavage reagent B and the caged active group A−C, allowing the former to subsequently trigger the bond cleavage of the latter to release its active group A *in situ*. However, currently available cleavage reagents would not be suitable for structural modification to mask the uncaging activity. In this regard, searching for a novel cleavage reagent which could be used to construct masked-B-A-C is urgently needed for bioorthogonal chemistry.

Given the extensive applications of the transition-metal palladium (Pd)-mediated bioorthogonal chemical reactions, we had successfully developed a group of O^2-propargylated diazeniumdiolates as a new class of bioorthogonal cleavage reaction-based nitric oxide (NO) prodrugs, which can be effectively uncaged in the presence of Pd(0) within living cells.[26] Since Pd and platinum (Pt) belong to the same transition-metal family, we further hypothesized that Pt may have catalytic properties similar to that of Pd. Accordingly, we selected some common Pt compounds including $PtCl_2$, $PtCl_4$, Pt(II) compounds cisplatin (**1**) and carboplatin (**2**), and Pt(IV) derivatives diamine trichloro hydroxy platinum (**3**) and (trimethyl)methylcyclopentadienyl platinum (**4**) to investigate the depropargylation efficiency on *O*-propargyl 4-methylumbelliferone (compound **5a**)[12] by spectrofluorometry- and high-performance liquid chromatography (HPLC)-based methods. Interestingly, we found that Pt(II) **1** effectively catalyzed the

https://dx.doi.org/10.1021/acs.jmedchem.0c01435
J. Med. Chem. XXXX, XXX, XXX−XXX

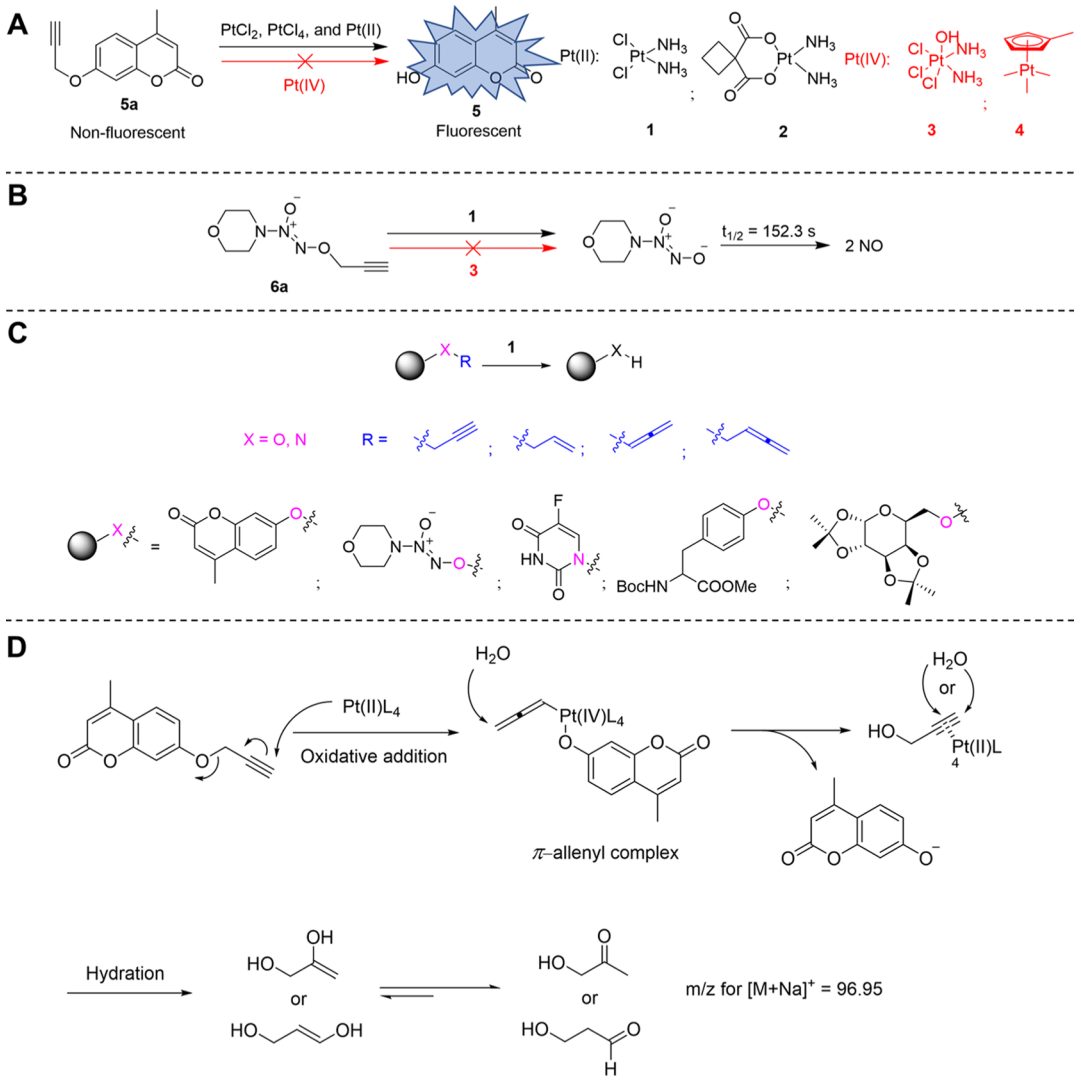

Figure 2. (A) Depropargylation reaction of non-fluorescent **5a** to generate highly fluorescent **5** in the presence of equal concentration of Pt compounds in phosphate-buffered saline (PBS), pH 7.4, containing 5% DMSO, at 37 °C. (B) **1**, a representative Pt(II), but not its Pt(IV) complex **3**, effectively triggered the depropargylation reaction of **6a** in PBS pH 7.4, containing 5% dimethyl sulfoxide (DMSO), at 37 °C to release NO. (C) **1**-triggered deprotections of *O*/*N*-propargyl/allyl/1,2-allene-yl/1,2-butadiene-yl from 4-methylumbelliferone, morpholine diazeniumdiolate, 5-fluoracil, *N*-boc-L-tyrosine methyl ester, and 1,2: 3,4-di-*O*-isopropylidene-D-galactopyranose. (D) Proposed mechanism for Pt(II)-catalyzed depropargylation reactions.

depropargylation of **5a**, whereas Pt(IV) **3** was not able to catalyze the same reaction (Figure 1C).

As it is known, some Pt(IV) complexes, such as ormaplatin, iproplatin, satraplatin, and so forth,[27] are kinetically inert platinum prodrugs under clinical trials and can be converted to active Pt(II) upon reduction by high concentrations of cytoplasmic reductants such as ascorbic acid in cancer cells, thus exhibiting increased toxicity to cancer cells.[28−34] In this regard, Pt(IV) **3** could act as a masked cleavage reagent (masked-B) and the hydroxyl group could be used for further coupling with the caged active agents (A−C) to produce a novel class of integrated bioorthogonal cleavage reaction-based prodrug (masked-B-A-C, Figure 1B). NO is a potential cancer therapeutic agent and several kinds of NO donors (diazeniumdiolate, furoxans, etc.) have been proven to possess potent antiproliferative activity against cancer cells.[35−38] Furthermore, the synergistic effect of NO and **1** in cancer therapy has been well described.[39−41] Given the concept of integrated bioorthogonal prodrug (masked-B-A-C) and the findings that Pt (II) **1**, but not Pt(IV) **3**, can trigger *O*-depropargylation, we design the first generation of integrated bioorthogonal prodrug **16**, in which the hydroxyl group of **3** and the hydroxyl group of the O^2-propargyl *N*-methylethanolamine diazeniumdiolate are connected via a succinic acid moiety (Figure 1D). We propose that **16** may be metabolically stable without intermolecular bioorthogonal reactions but could be specifically reduced by cytoplasmic reductants in cancer cells, rather than in normal cells, to release **1** and O^2-propargyl caged diazeniumdiolate moiety. The former then catalyzes the bond cleavage of *O*-propargyl in the latter to liberate large amounts of NO *in situ*, together with **1**, generating selective and synergistic antiproliferative activity against cancer cells, while sparing normal cells (Figure 1D).

Herein, we first study the chemistry of Pt-derived cleavage reactions of *O*/*N*-propargyl in a range of molecules including a fluorophore, an anticancer drug 5-fluoracil, tyrosine, NO donor diazeniumdiolates, and a monosaccharide. The target compound **16**, its moieties, and analogue are then synthesized, and the bioorthogonal cleavage reactions in cell-free solutions are

https://dx.doi.org/10.1021/acs.jmedchem.0c01435
J. Med. Chem. XXXX, XXX, XXX−XXX

Scheme 1. Synthetic Route of 16 and 17

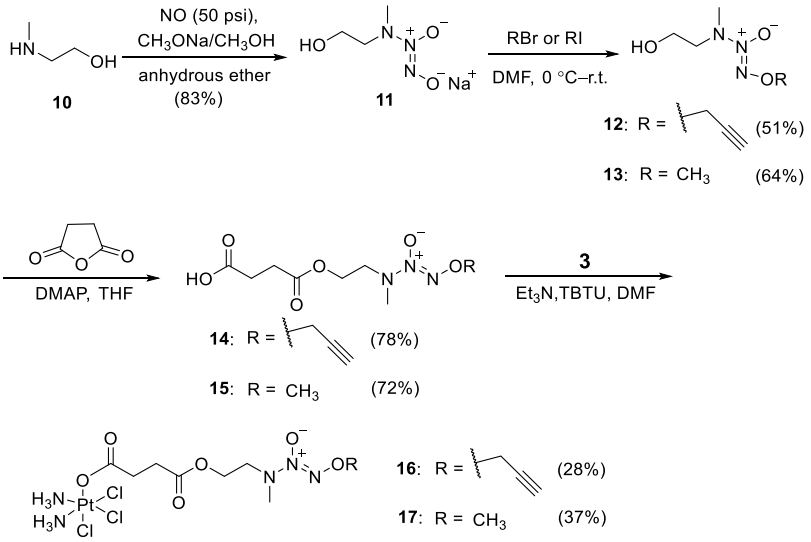

investigated. NO-release behaviors, Pt accumulation properties, and cancer cell growth inhibitory activity are further investigated in normal and cancer cells as well as in zebrafish.

RESULTS AND DISCUSSION

Chemistry of Pt-Derived Cleavage Reactions of *O*/*N*-Propargyl. We first selected some common platinum compounds including $PtCl_2$, $PtCl_4$, Pt(II) compounds cisplatin (**1**) and carboplatin (**2**), and Pt(IV) derivatives diamine trichloro hydroxy platinum (**3**) and (trimethyl) methylcyclopentadienyl platinum (**4**) to investigate the depropargylation efficacy on non-fluorescent *O*-propargyl 4-methylumbelliferone (compound **5a**) to generate highly fluorescent **5** by using $Pd(dba)_2$ as a positive control via fluorometry (Figure S1) and HPLC assays (Figure S2). It was found that $PtCl_2$ and $PtCl_4$ effectively triggered the depropargylation of **5a** to generate **5**, superior to $Pd(dba)_2$. Interestingly, Pt(II) **1** exhibited more catalytic activity than **2**, whereas Pt(IV) **3** and **4** were not able to catalyze the depropargylation reaction of **5a** (Figure 2A). Different from the excellent work by Bernardes's research group which involved platinum complexes [K_2PtCl_4 or **1**]-triggered bond-cleavage amide and *N*-propargyl for drug activation,[19] our parallel work found that Pt(IV) complexes **3** and **4** were not able to trigger the cleavage of *O*/*N*-propargyl. Furthermore, it was found that **1** effectively triggered the depropargylation of O^2-propargyl-1-(*N*,*N*-morpholine)-diazeniumdiolate **6a**[25,26] to generate NO (presented as nitrite), while **3** was not able to trigger this reaction (Figures 2B and S3). To study the scope of **1**-triggered cleavage reactions, *O*-propargyl/allyl/1,2-allene-yl/1,2-butadiene-yl were respectively introduced to the hydroxyl group of **5**. As shown in Table S1, **1** effectively stimulated the deprotection of *O*-propargyl (**5a**) and 1,2-butadiene-yl (**5d**) with converted yields of **5** as 76 and 79%, respectively, superior to the deprotection of *O*-allyl (**5b**) and 1,2-allene-yl (**5c**). To further extend the substrates, *O*/*N*-propargyl/allyl were introduced to a range of molecules including morpholine diazeniumdiolate **6**, 5-fluoracil **7**, *N*-boc-L-tyrosine methyl ester **8**, and a monosaccharide 1,2:3,4-di-*O*-isopropylidene-D-galactopyranose **9**. Excitingly, **1** effectively triggered the deprotection of *N*-propargyl (**7a**) and allyl (**7b**) from 5-fluoracil with converted yields as 66 and 92%, respectively. Importantly, **1** was also able to deprotect propargyl and allyl from O^2 position in morpholine diazeniumdiolate (**6a**, **6b**), the phenolic hydroxyl group in tyrosine (**8a**, **8b**), and the hydroxyl group in galactose (**9a**, **9b**), indicating its extensive catalytic scope (Figure 2C).

Next, we investigated the effects of temperature (Figure S4A), water (Figure S4B), and pH values (Figure S4C) on the **1**-triggered depropargylation to reveal the underlying mechanism. It was found that the reaction rate of **1**-triggered depropargylation at 37 °C was significantly greater than that at 25 °C, and water was essential for this reaction. Meanwhile, pH 7.4 and 6.6 were preferred for the depropargylation, superior to the alkaline condition, suggesting the desired biocompatibility of **1**-triggered depropargylation reaction. Given that hydroxyacetone or 3-hydroxypropanal was detected in the reaction mixture by liquid chromatography–mass spectrometry (LC–MS) (Figure S5) and the mechanism of Pd-triggered depropargylation was previously reported,[9] we proposed one plausible mechanism of **1**-triggered depropargylation. As shown in Figure 2D, **1**, as a four-coordinate complex with unsaturated coordination on Pt atom, could coordinate with *O*-propargyl group of compound **5a** in H_2O to trigger the bond cleavage reaction the same as Pd, whereas Pt(IV) **3**, a saturated coordination complex, may not be able to react with propargyl group to trigger the depropargylation reaction.

Synthesis of Integrated Bioorthogonal Prodrug 16 and Its Analogue 17. The synthetic route of target compound **16** and its O^2-methyl analogue **17**, in which the O^2-methyl group could not be deprotected by Pt(II), is depicted in Scheme 1. Briefly, the reaction of NO gas (50 psi) with *N*-methylethanolamine (**10**) in the presence of NaOMe in dry ether offered diazeniumdiolates sodium salt **11**, which was subsequently treated with propargyl bromide or iodomethane to produce O^2-propargyl **12** and O^2-methyl **13**, respectively. Then **12** and **13** were individually treated with succinic anhydride to furnish **14** and **15**. Finally, the reactions of **14** or **15** with **3** in the presence of TBTU in dimethylformamide (DMF) generated the target compounds **16** and **17**, respectively.

Degradation and the NO-Release Behaviors of 16 and Related Compounds in Cell-Free System. The degradation and the NO-release behaviors of **16** and **17** in blank PBS (pH = 7.4, 37 °C) or in PBS-containing molar equivalent L-(+)-ascorbic acid were first investigated by using HPLC and Griess assays, respectively.[42] As shown in Figure 3A, both **16** and

https://dx.doi.org/10.1021/acs.jmedchem.0c01435
J. Med. Chem. XXXX, XXX, XXX–XXX

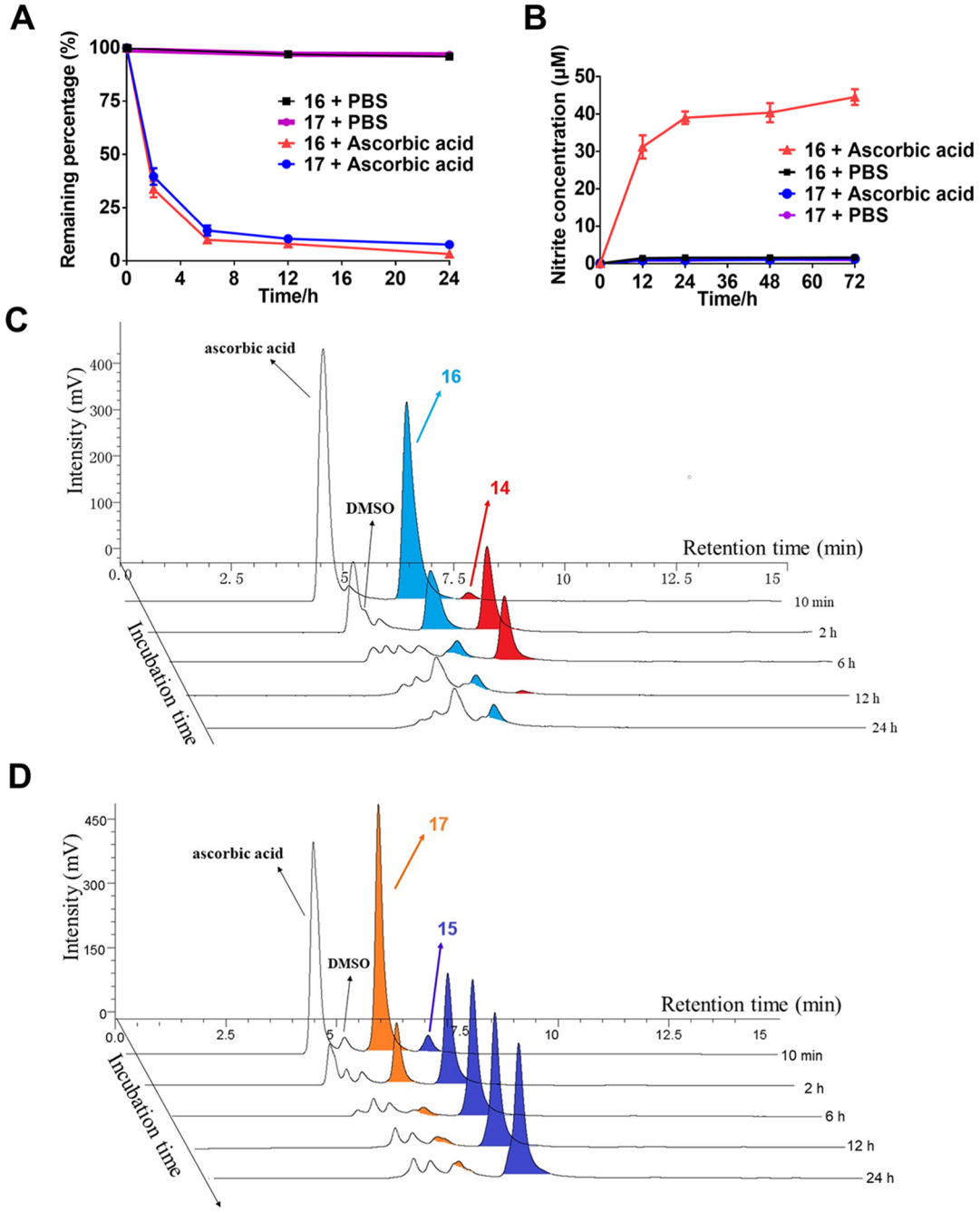

Figure 3. (A) Decomposition kinetics of **16** and **17** (the initial concentration of the test compounds was 500 μM) and (B) NO-release behaviors of **16** and **17** (the initial concentration of the test compounds was 125 μM) in the presence or absence of molar equivalent concentration of L-(+)-ascorbic acid in PBS (pH = 7.4, 37 °C). Error bars represent ±SD from three independent experiments. (C) HPLC analysis of ascorbic acid (500 μM)-mediated degradation of **16** (500 μM) and D) HPLC analysis of ascorbic acid (500 μM)-mediated degradation of **17** (500 μM) in PBS solution containing 5% DMSO (pH = 7.4, 37 °C).

17 were stable in PBS after incubation for 24 h but rapidly degraded in the presence of molar equivalent ascorbic acid. Furthermore, it was found that with ascorbic acid, **16** was first degraded to generate O^2-propargyl diazeniumdiolate moiety **14** which was gradually exhausted to release up to 44.6 μM of nitrite anion (an oxidative metabolite of NO) after incubation for 72 h (Figure 3B,C). In sharp contrast, **17** was reduced by ascorbic acid to generate O^2-methyl diazeniumdiolate moiety **15**, while it was stable without further NO release (Figure 3B,D). Besides, the degradation and the NO-release behaviors of **14** and **15** in the presence of molar equivalent **1**, **3**, **3** + ascorbic acid in PBS (pH = 7.4, 37 °C) were studied (Figure S6). It was found that both **1** and **3** + ascorbic acid effectively triggered the degradation of **14** to liberate a considerable amount of NO, whereas **3** alone did not catalyze the degradation of **14**. Expectedly, neither **1** nor **3** triggered the demethylation of **15**. To sum up, these data preliminarily revealed the proposed bioorthogonal degradation route of **16**, that is, **16** was first reduced by ascorbic acid to liberate **1** and **14**, and then **1** catalyzed the bond cleavage of O^2-propargyl moiety in **14** to produce the diazeniumdiolate anion, which spontaneously released two molecules of NO.

https://dx.doi.org/10.1021/acs.jmedchem.0c01435
J. Med. Chem. XXXX, XXX, XXX−XXX

Antiproliferative Activity of 16 and Related Compounds Against A2780 and IOSE80 Cells. We then investigated the antiproliferative activity of Pt(II) **1** and Pt(IV) **3**, NO donor moieties **14**, **15**, **3** + **14** (1:1), and **3** + **15** (1:1), as well as the target compound **16** and its O^2-methyl analogue **17** against human ovarian cancer A2780 cells and human normal ovarian epithelial IOSE80 cells by MTT assay. As shown in Table 1, compound **14** exhibited very weak antiproliferative activity against both A2780 and IOSE80 cells, while the pretreatment of **3** for 10 h significantly enhanced the antiproliferative activity of **14** against A2780 cells (89.46 ± 4.87 μM for **14** alone vs 0.81 ± 0.07 μM for **3** + **14**), indicating **3** could enter the cancer cells and be reduced to form **1** to further trigger the cleavage of O^2-propargyl, releasing a large amount of NO in living cancer cells. Importantly, integrated prodrug **16** exhibited more potent antiproliferative activity (0.23 ± 0.01 μM) against A2780 cells superior to **1** (1.08 ± 0.06 μM), **3** (1.69 ± 0.09 μM) and **3** + **14** (0.81 ± 0.07 μM). Additionally, **16** showed much improved safety to normal epithelial IOSE80 cells with selective factor (SF: 518) relative to **1** (SF: 7.8) and **3** (SF: 10.9), indicating desirable biocompatibility of the integrated prodrug. One plausible explanation is that as a derivative of **3**, **16** possesses greater steric hindrance and thus more stability in normal cells. As expected, compared to **16**, its O^2-methyl analogue **17**, which was not able to be uncaged to liberate NO, exhibited weaker antiproliferative activity against A2780 cells, indicating the potential synergistic effect of NO and Pt(II).

Table 1. IC_{50} Values (μM) of the Integrated Prodrug 16 and Its Analogue and Fragments[a]

compounds	A2780	IOSE80	SF[c]
1	1.080 ± 0.06	8.420 ± 0.57	7.80
3	1.690 ± 0.09	18.47 ± 1.36	10.9
14	89.46 ± 4.87	186.4 ± 10.27	2.10
15	103.9 ± 7.54	212.1 ± 12.04	2.00
14 + **3**[b]	0.8100 ± 0.07	137.6 ± 7.94	10.0
15 + **3**[b]	23.50 ± 1.38	164.8 ± 9.15	7.00
16	0.2300 ± 0.01	119.1 ± 7.98	518
17	0.8300 ± 0.05	88.28 ± 4.86	106

[a]Human ovarian cancer A2780 cells and human normal ovarian epithelial IOSE80 cells were treated with the indicated compounds for 72 h, and the cell viability and IC_{50} values were determined by MTT assay. Data were expressed as the mean ± SD from three individual experiments. [b]The cells were incubated with **3** for 10 h, followed by being rinsed and resuspended with **14** or **15** under the same concentrations for 72 h, and the IC_{50} values were assessed by MTT assay. [c]The SF is defined as the IC_{50} value against IOSE80 cells/IC_{50} value against A2780 cells.

NO-Release Behaviors of 16 and Related Compounds in A2780 and IOSE80 Cells. Next, we examined the NO-release behaviors of the integrated prodrug **16**, its analogue **17**, and the NO donor fragments **14** and **15** in A2780 cells and IOSE80 cells by using a well-known NO-sensitive fluorophore probe 4-amino-5-(methylamino)-2′,7′-difluorofluorescein diacetate (DAF-FM DA)[43] and JS-K (a well-known Glutathione S-transferase (GST)-activated NO donor prodrug)[44] as a positive control. As shown in Figures 4A and S7A,B, NO donor moieties **14** or **15** alone (0.23 μM, for 8 h) generated very low fluorescence in both normal epithelial IOSE80 cells and ovarian cancer A2780 cells as that of the blank control, while the pretreatment of the same concentration of **3** for 10 h significantly increased the relative mean fluorescence intensity (MFI) of **14**, but not **15**, in cancer A2780 cells rather than in normal epithelial IOSE80 cells, suggesting that Pt(II)-induced O^2-depropargylation reaction possesses desirable selectivity for cancer cells. Interestingly, the treatment of **16** (0.23 μM, for 8 h) generated the highest relative MFI as 25.33 in cancer A2780 cells, superior to **14** plus **3** (15.16) and JS-K (7.75), indicating that the integrated prodrug could more effectively accumulate in cancer cells than separated administration, and Pt(II)-induced O^2-cleavage reaction may be more effective than enzymatic O^2-deprotection which is GST enzyme-activity- and concentration-

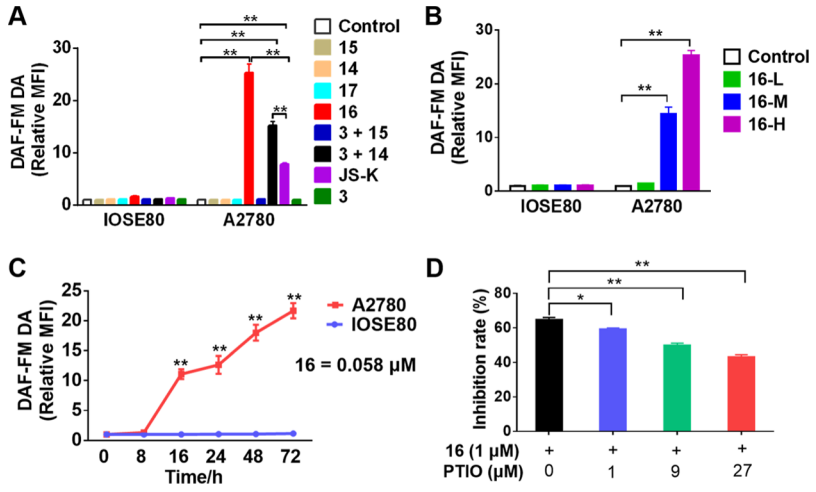

Figure 4. (A) NO-release behaviors of the test compounds (0.23 μM) in the cells. A2780 and IOSE80 cells were treated with the indicated concentrations of the test compounds for 8 h, then stained with DAF-FM DA ($\lambda_{ex/em}$ = 495/515 nm), and analyzed by fluorescence-activated cell sorting (FACS). For **3** + **14** and **3** + **15** groups, the cells were first treated with **3** at indicated concentrations for 10 h, followed by being rinsed and resuspended with the equimolar concentrations of **14** or **15** for additional 8 h, then analyzed as mentioned above. (B) NO released by **16** at different concentrations (16-L: 0.058, 16-M: 0.115, and 16-H: 0.23 μM) for 8 h in the cells. (C) NO released by **16** (0.058 μM) with different incubation times (0, 8, 16, 24, 48, and 72 h) in the cells. (D) Effects of NO scavenger carboxy-PTIO (PTIO) on the A2780 cell growth inhibitory activity of **16**. A2780 cells were pretreated with PTIO (0, 3, 9, and 27 μM) for 1 h, followed by being rinsed and resuspended with **16** (1 μM) for 24 h, and the cell viability was determined by MTT assay. Data are expressed as the mean ± SD from three independent experiments (n = 3): $^{**}P < 0.01$, $^{*}P < 0.05$.

https://dx.doi.org/10.1021/acs.jmedchem.0c01435
J. Med. Chem. XXXX, XXX, XXX−XXX

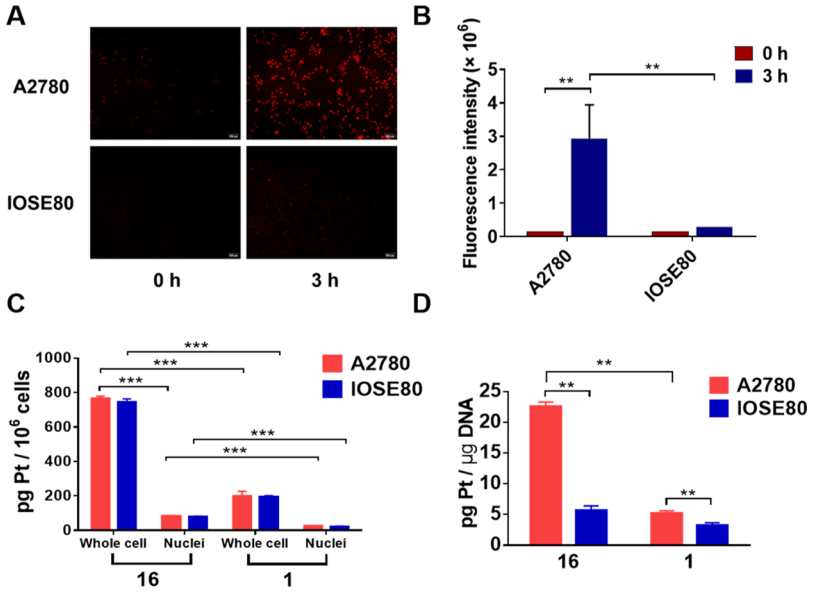

Figure 5. (A) Representative confocal microscopy images of A2780 cells and IOSE80 cells. The cells were treated with **16** (30 μM) for 3 h, then washed and stained with RDC1 (20 μM) for another 4 h ($\lambda_{ex/em}$ = 400/565 nm, ZEN 2012 software was used to set as red). (B) Quantification of fluorescence intensity for the cells in each group after staining with RDC1 for 0 and 3 h. Data are the mean ± SD from four independent experiments (n = 4). $^{**}P < 0.01$. (C) Cellular and nuclei Pt accumulation of **16** and **1** (5 μM) incubated with A2780 (red) and IOSE80 (blue) cells for 24 h. (D) Platination levels of nuclear DNA following a 24 h incubation of the complexes (5 μM) with A2780 (red) and IOSE80 (blue) cells. Data are the mean ± SD from three independent experiments (n = 3): $^{***}P < 0.001$, $^{**}P < 0.01$.

dependent.[45] In addition, **16** generated NO in dose- and time-dependent manners in cancer A2780 cells (Figures 4B,C and S7C,D). Interestingly, the pretreatment of NO scavenger carboxy-PTIO partially counteracted the A2780 cell growth inhibitory activity of **16** in a dose-dependent manner (Figure 4D). These results together with the antiproliferative data above clearly demonstrated that integrated Pt(IV) derivative **16** was preferably reduced in cancer cells to generate Pt(II) moiety, which initiated the O^2-cleavage reaction to spontaneously release NO *in situ*, generating synergistic and potent antiproliferative activity against cancer cells, while sparing normal cells.

Pt(II) Release, Cellular Accumulation, and Binding to Nuclear DNA of 16 in A2780 and IOSE80 Cells. We then used a ratiometric probe RDC1,[46] which was reported to be able to distinguish between Pt(II) **1** and its Pt(IV) derivatives, to investigate **1** generation after the treatment of **16** in both A2780 and IOSE80 cells. First, **16** (30 μM) was incubated with A2780 and IOSE80 cells for 3 h. The cells were washed and resuspended with RDC1 (20 μM) for another 4 h. Confocal microscopy was used to observe the fluorescence intensity of the cells. As shown in Figure 5A,B, **16** significantly produced **1** in A2780 cells, whereas a little **1** was generated in normal IOSE80 cells, indicating that the Pt(IV) complex **16** could be preferably reduced in cancer cells to generate **1**. Notably, **1** derived from **16** has two functions: one is as a cleavage reagent to trigger NO release, and the other is as a cytotoxin via binding DNA. To identify the spatiotemporal functions of **1** derived from **16**, we studied the cellular Pt uptake, nuclear accumulation, and nuclear DNA platination of **16** in the cells by using **1** as a control. Briefly, A2780 and IOSE80 cells were respectively treated with **16** (5 μM) or **1** (5 μM) for 24 h. Then the cell nuclei were separated by Nuclei EZ Prep kit, and the whole cellular Pt and nuclei Pt concentrations (expressed as pg Pt/10^6 cells) were measured by graphite furnace atomic absorption spectrometry (GF-AAS) analysis.[47−50] Meanwhile, the nuclear DNA was extracted and purified by the spin column quantification kit (Qiagen, Valencia, CA), and the nuclear DNA platination levels (expressed as pg Pt/μg DNA) were measured by using the same assay. As shown in Figure 5C, **16** exhibited much more improved accumulation pattern than **1** in whole cells and in nuclei in both cancer and normal cells. For example, after treatment with **16** for 24 h, A2780 cells had 763.53 ± 14.81 pg Pt/10^6 in whole cells and 84.4 ± 1.77 pg Pt/10^6 cells in nuclei, while A2780 cells had only 98.34 ± 23.00 pg Pt/10^6 in whole cells and 24.78 ± 1.55 pg Pt/10^6 cells in nuclei after treatment with **1** for 24 h. One plausible reason is that **16** bearing two axial ligands has higher lipophilicity and thus possesses improved cell penetrating ability relative to **1**, which was approved by the measured Log$P$ value of **16** (−0.89) compared to the reported Log$P$ value of **1** as −2.25 by the same method.[30,47,51] Importantly, **16** exhibited significant nuclear DNA platination levels (22.56 pg Pt/μg DNA) superior to that of **1** (5.18 pg Pt/μg DNA) in A2780 cells (Figure 5D). Overall, these results demonstrated that **16** effectively penetrated cancer cells and then was reduced by cytoplasmic reductants to liberate **1** and NO donor moiety. After the cleavage reaction was triggered by **1**, it was able to platinate nuclear DNA, together with NO, generating selective, synergistic, and potent antiproliferative activity against cancer cells.

Anticancer Activity and NO-Release Behavior of 16 in a Zebrafish Embryo Model. Having established that **16** can generate **1** and release NO, exerting selective and potent antiproliferation activity against A2780 cells, we aimed to demonstrate that **16** could be activated in cancer cells *in vivo* and inhibit cancer cell growth in a zebrafish embryo model.[15,52−55] First, Dil-labeled A2780 cells were microinjected into the yolk sac of zebrafish embryos to establish the xenograft model. After 24 h, **16** (5% DMSO in water, final concentration 1 μM), blank solution, and **1** (5% DMSO in water, final concentration 1 μM) were incubated with zebrafish in a 6-well plate at 37 °C for 72 h. Images of the zebrafish were acquired at 0 and 72 h after incubation (Figure 6A). As shown in Figure S8A, all groups were

https://dx.doi.org/10.1021/acs.jmedchem.0c01435
J. Med. Chem. XXXX, XXX, XXX−XXX

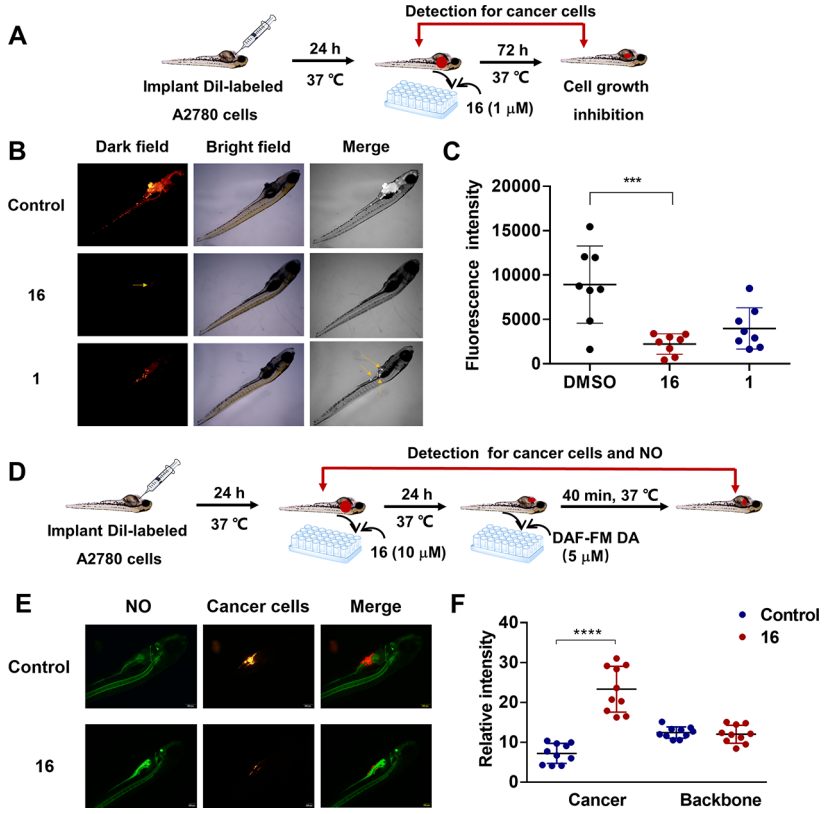

Figure 6. (A) Schematic illustration of the assay to evaluate the anticancer activity of **16** in zebrafish implanted with Dil-labeled A2780 cells ($\lambda_{ex/em}$ = 553/570 nm, ZEN 2012 software was used to set as red). (B) Representative confocal microscopy images of the zebrafish for each group at 72 h. (C) Quantification of fluorescence intensity of the implanted cancer cells for each group at 72 h (n = 8), ***P < 0.001 vs blank control. (D) Schematic illustration of the dual-imaging assay. (E) Representative confocal microscopy images of the zebrafish for each group at 40 min after the addition of DAF-FM DA ($\lambda_{ex/em}$ = 495/515 nm, ZEN 2012 software was used to set as green). (F) Quantification of the fluorescent intensity in the location of the implanted cancer cells and backbone of the zebrafish at 40 min after the addition of DAF-FM DA (n = 10), ****P < 0.0001 vs blank control.

successfully implanted with Dil-labeled A2780 cells. The fish in **16** group exhibited significantly lower fluorescence intensity with an inhibitory rate of 75.03% than those in blank control, and also superior to **1** with an inhibitory rate as 55.38%, suggesting potent anticancer activity of **16** in zebrafish (Figure 6B,C). To further confirm that NO release could be specific in cancer cells, we designed a dual-imaging assay (Figure 6D). Briefly, zebrafish implanted with Dil-labeled A2780 cells were incubated with **16** (5% DMSO in water, final concentration 10 μM) in a 6-well plate at 37 °C for 24 h, followed by being collected, washed, and re-incubated with NO probe DAF-FM DA (5% DMSO in water, final concentration 5 μM) for additional 40 min. Images were acquired at 0 h before **16** treatment and 40 min after DAF-FM DA incubation for both cancer cells and NO (Figure 6D). As shown in Figure S8B, at 0 h before **16** treatment, the fish had been successfully implanted with Dil-labeled A2780 cells and did not show any fluorescence of NO without NO probe. After DAF-FM DA incubation, as shown in the panel of merge in Figure 6E, the location of NO overlapped that of the cancer cells, and **16** group exhibited significantly higher fluorescence of NO in cancer cells (3.24-fold, P < 0.0001) than the blank control group (Figure 6F). Interestingly, in the backbone of zebrafish, fluorescence of NO in **16** group was comparable with that in the blank control group. These results clearly demonstrated that **16**, as an integrated and inert prodrug, could be stable *in vivo* after oral administration but specifically reduced in the implanted human ovarian cancer cells to liberate **1** (cleavage reagent) and O^2-propargyl diazeniumdiolate (caged active group). The former triggered the cleavage of O^2-propargyl in the latter to release a large amount of NO *in situ*, generating potent cancer cell growth inhibitory activity in zebrafish.

CONCLUSIONS

In conclusion, to address the shortcomings of current bioorthogonal cleavage chemistry, we proposed, for the first time, a strategy of direct modification of cleavage reagents (masked-B) and integrated bioorthogonal cleavage reaction-based prodrug (masked-B-A-C). We found a new class of Pt(II)-triggered bioorthogonal cleavage reactions in which Pt(II) but not Pt(IV) complexes effectively triggered the cleavage of *O*/*N*-propargyl in various molecules including a fluorophore, NO donor diazeniumdiolates, an anticancer drug 5-fluorouracil, tyrosine, and a monosaccharide under biocompatible conditions with good yields. Based on this interesting discovery, an integrated bioorthogonal cleavage reaction-based prodrug **16**, as a proof-of-concept, was rationally designed, feasibly synthesized, and biologically evaluated. This integrated bioorthogonal prodrug, **16**, bearing both a masked cleavage reagent [Pt(IV) moiety] and a caged active group (O^2-propargyl *N*-methylethanolamine diazeniumdiolate), efficiently entered cancer cells and was specifically reduced by cytoplasmic reductants in cancer cells to release Pt(II) **1** and O^2-propargyl-caged diazeniumdiolate moiety. Depropargylation of the O^2 position triggered by **1** generated diazeniudiolates anions, which spontaneously released an abundance of NO *in situ*. Additionally, **1** was able to

https://dx.doi.org/10.1021/acs.jmedchem.0c01435
J. Med. Chem. XXXX, XXX, XXX−XXX

platinate nuclear DNA, together with NO, generating selective, synergistic, and potent antiproliferative activity against cancer cells. Although Pt(II) is toxic to cells, the depropargylation reaction selectively occurred in cancer cells and thus was biocompatible to normal cells. Notably, **16** exhibited more potent antiproliferative activity against human ovarian cancer A2780 cells and much lower toxicity to human normal ovarian epithelial IOSE80 cells than **1**, which is a front-line chemotherapy for ovarian cancer.[56] Significantly, in a xenograft model in zebrafish, **16** was specifically activated in the implanted A2780 cells to release NO *in situ*, generating potent cancer inhibitory activity. **16** possesses potential developability and will be investigated for anticancer activity in mice and other preclinical studies, and the corresponding results will be reported in due course.

Taken together, the fact that Pt(II) **1**, but not its Pt(IV) complex **3**, triggers *O/N*-depropargylation reactions gives us a chance to realize the strategy of integrated bioorthogonal cleavage reaction-based prodrugs bearing both a masked cleavage reagent and caged active group within one small molecule and possessing controllable drug activation in cancer cells *in vivo*. Meanwhile, this integration strategy could be flexibly expanded to other active molecules of interest. Thus, the new **1**-triggered depropargylation reaction and novel integrated bioorthogonal chemistry-based prodrug strategy may promote diverse applications in chemical biology and inspire further research in bioorthogonal chemistry.

EXPERIMENTAL SECTION

General Methods. All reagents and solvents were bought from commercial suppliers and used as received without further drying or purification. NO gas was purchased from Nanjing TIANZE GAS Co., Ltd. Melting points were determined on a MelTEMP II melting point apparatus. ^{1}H NMR (300 or 500 MHz) and ^{13}C NMR (75 or 125 MHz) spectra were recorded with Bruker Avance 300 and 500 MHz spectrometers at 303 K, using tetramethylsilane as an internal standard. Mass and high-resolution mass spectrometry (HRMS) spectra were obtained on an Agilent Q-TOF 6520 or Waters Synapt G2-S spectrometer. Analytical and preparative thin-layer chromatography was performed on silica gel (200−300 mesh) GF/UV 254 plates, and the chromatograms were visualized under UV light at 254 nm. Analytical reversed-phase HPLC (RPLC) was conducted on a Shimadzu Prominence HPLC system using Innovai ODS-2 column (5 μm, 100 Å, 150 or 250 × 4.60 mm). Test compounds **14**−**17** with a purity of >95% were used for biological experiments.

*Synthesis of Diamine Trichloro Hydroxy Platinum (**3**).* Diamine trichloro hydroxy platinum (**3**) was synthesized by the reaction of cisplatin (**1**) with *N*-chlorosuccinimide (NCS) as previously reported.[57,58] Briefly, NCS (1.0 equiv), cisplatin (1.0 equiv), and H_2O (20 mL) were added to a 100 mL round-bottom flask, and the reaction was stirred at room temperature for 5 h in the dark. The solid residue was removed by centrifugation, and the filtrate was evaporated to dryness to get a pale-yellow solid that was washed with ethanol and diethyl ether to furnish **3** as a light yellow solid. Yield 87.6%. ^{1}H NMR (300 MHz, DMSO-d_6): δ 5.38−6.02 (m, 6H). MS (ESI) *m/z*: $Cl_3H_7N_2OPt$, $[M + H]^+$ = 351.9.

*Synthesis of O-Propargyl 4-Methylumbelliferone (**5a**).* 4-Methylumbelliferone (200 mg), propargyl bromide (4.0 equiv), and K_2CO_3 (4.0 equiv) were dissolved in acetone (10 mL). The obtained solution was stirred at 60 °C for 12 h. After the reaction mixture was cooled and the solvent was removed by evaporators, the residue was treated with H_2O (15 mL) and extracted with ethyl acetate (EA) (15 mL × 3). The organic phase was washed with water, dried over Na_2SO_4, and evaporated under vacuum. The crude product was purified by using flash column chromatography to give compound **5a** (210 mg, 86%). ^{1}H NMR (300 MHz, $CDCl_3$): δ 7.52 (d, *J* = 9.6 Hz, 1H), 6.94−6.91 (m, 2H), 6.15 (s, 1H), 4.76 (d, *J* = 2.1 Hz, 2H), 2.57 (t, *J* = 2.4 Hz, 1H), and 2.40 (s, 3H).

*Synthesis of O-Allyl 4-Methylumbelliferone (**5b**).* 4-Methylumbelliferone (200 mg), allyl bromide (4.0 equiv), and K_2CO_3 (4.0 equiv) were dissolved in acetone (10 mL). The solution was stirred at 60 °C for 12 h. After the reaction mixture was cooled and the solvent was removed by evaporators, the residue was treated with H_2O (15 mL) and extracted with EA. The organic phase was washed with water, dried over Na_2SO_4, and evaporated under vacuum. The crude product was purified by using flash column chromatography to give compound **5b** (218 mg, 89%). ^{1}H NMR (300 MHz, $CDCl_3$): δ 7.49 (d, *J* = 8.7 Hz, 1H), 6.90−6.82 (m, 2H), 6.13 (s, 1H), 6.10−5.98 (m, 1H), 5.47−5.32 (m, 2H), 4.60 (d, *J* = 5.4 Hz, 2H), and 2.39 (s, 3H).

*Synthesis of O-1,2-Allene-yl 4-Methylumbelliferone (**5c**).* Compound **5a** (200 mg) and *t*-BuOK (0.5 equiv) were dissolved in 5.0 mL of dry *t*-BuOH and stirred at 90 °C for 4 h. The reaction mixture was concentrated and purified by silica gel column chromatography (1:50, EA: hexanes) to give the title compound **5c** (32 mg, 16%). ^{1}H NMR (300 MHz, $CDCl_3$): δ 7.07 (d, *J* = 8.4 Hz, 1H), 6.58−6.49 (m, 3H), 5.85 (s, 1H), 5.36 (d, *J* = 1.5 Hz, 1H), 5.11 (s, 1H), and 2.09 (s, 3H).

*Synthesis of O-1,2-Butadiene-yl 4-Methylumbelliferone (**5d**).* Compound **5a** (200 mg), CuI (0.5 equiv), Cy_2NH (1.8 equiv) and paraformaldehyde (2.5 equiv) were dissolved in dry dioxane (5 mL) and refluxed for 3 h in a schlenk tube. The reaction mixture was concentrated and purified by silica gel column chromatography to give compound **5d** (105 mg, 49%). ^{1}H NMR (300 MHz, $CDCl_3$): δ 7.49 (d, *J* = 8.7 Hz, 1H), 6.88−6.83 (m, 2H), 6.13 (s, 1H), 5.42−5.33 (m, 1H), 4.92−4.89 (m, 2H), 4.65−4.61 (m, 2H), and 2.39 (s, 3H).

*Synthesis of O^2-Propargyl-1-(N,N-morpholine)-diazeniumdiolate (**6a**).* To a solution of *N,N*-morpholine diazeniumdiolates sodium salts (200 mg) in DMF (5 mL) at 0 °C under a steady stream of nitrogen was added dropwise propargyl bromide (1.0 equiv) in DMF (1 mL). The mixture was allowed to warm to room temperature and stirred overnight. Then the solvent was removed by an evaporator, and the obtained residue was treated with H_2O (20 mL) and extracted with EA (3 × 50 mL). The organic layers were combined and washed with brine (20 mL), dried over Na_2SO_4, and evaporated under vacuum. The crude product was purified by flash chromatography on silica gel using EA and hexane for eluting to give compound **6a** (166 mg, 76%). ^{1}H NMR (300 MHz, $CDCl_3$): δ 4.78 (d, *J* = 2.4 Hz, 2H), 3.84 (t, *J* = 4.8 Hz, 4H), 3.46 (t, *J* = 4.8 Hz, 4H), and 2.53 (t, *J* = 2.4 Hz, 1H).

*Synthesis of O^2-Allyl-1-(N,N-morpholine)-diazeniumdiolate (**6b**).* To a solution of *N,N*-morpholine diazeniumdiolates sodium salts (200 mg) in DMF (5 mL) at 0 °C under a steady stream of nitrogen was added dropwise allyl bromide (1.0 equiv) in DMF (1 mL). The mixture was allowed to warm to room temperature and stirred overnight. Then the solvent was removed by an evaporator, and the obtained residue was treated with H_2O (20 mL) and extracted with EA (3 × 50 mL). The organic layers were combined and washed with brine (20 mL), dried over Na_2SO_4, and evaporated under vacuum. The crude product was purified by flash chromatography on silica gel using EA and hexane for eluting to give compound **6b** (24 mg, 11%). ^{1}H NMR (300 MHz, $CDCl_3$): δ 6.13−5.86 (m, 1H), 5.45−5.23 (m, 2H), 4.69 (d, *J* = 6.0 Hz, 2H), 3.84 (t, *J* = 4.8 Hz, 4H), and 3.41 (t, *J* = 4.8 Hz, 4H).

*Synthesis of N-Propargyl 5-Fluorouracil (**7a**).* To a stirred solution of 5-fluorouracil (200 mg) in anhydrous DMF, K_2CO_3 (1.0 equiv) was added and stirred for 30 min. Then propargyl bromide (1.1 equiv) was added to the mixture and allowed to stir at 50 °C for 12 h. After the removal of the solvent by evaporating under reduced pressure, the residue was purified by silica gel column chromatography to give compound **7a** (100 mg, 39%). ^{1}H NMR (300 MHz, DMSO-d_6): δ 11.89 (s, 1H), 8.11 (d, *J* = 6.3 Hz, 1H), 4.46 (s, 2H), and 3.42 (s, 1H).

*Synthesis of N-Allyl 5-Fluorouracil (**7b**).* To a stirred solution of 5-fluorouracil (200 mg) in anhydrous DMF, K_2CO_3 (1.0 equiv) was added and stirred for 30 min. Then allyl bromide (1.1 equiv) was added to this mixture and allowed to stir at 50 °C for 12 h. After the removal of the solvent by evaporating under reduced pressure, the residue was purified by silica gel column chromatography to give compound **7b** (124 mg, 47%). ^{1}H NMR (500 MHz, DMSO-d_6): δ 11.78 (s, 1H), 8.01

https://dx.doi.org/10.1021/acs.jmedchem.0c01435
J. Med. Chem. XXXX, XXX, XXX−XXX

(d, J = 11.5 Hz, 1H), 5.94−5.81 (m, 1H), 5.21−5.14 (m, 2H), and 4.24 (d, J = 8.5 Hz, 2H).

*Synthesis of O-Propargyl N-Boc-L-tyrosine Methyl Ester (**8a**).* *N*-Boc-L-tyrosine methyl ester (200 mg), propargyl bromide (4.0 equiv), and K_2CO_3 (4.0 equiv) were dissolved in acetone (10 mL). The solution was stirred at 60 °C for 12 h. After the reaction mixture was cooled and the solvent was removed by evaporators, the residue was treated with H_2O (15 mL) and extracted with EA. The combined organic layers were washed with water, dried over Na_2SO_4, and evaporated by vacuum. The crude product was purified using flash column chromatography to give compound **8a** (132 mg, 59%). ^{1}H NMR (300 MHz, $CDCl_3$): δ 7.05 (d, J = 8.7 Hz, 2H), δ 6.90 (d, J = 8.7 Hz, 2H), 4.94 (s, 1H), 4.66 (d, J = 2.4 Hz, 2H), 4.54 (d, J = 6.9 Hz, 1H), 3.71 (s, 3H), 3.03 (t, J = 6.0 Hz, 2H), 2.51 (t, J = 2.4 Hz, 1H), and 1.41 (s, 9H).

*Synthesis of O-Allyl N-Boc-L-tyrosine Methyl Ester (**8b**).* *N*-Boc-L-tyrosine methyl ester (200 mg), allyl bromide (4.0 equiv), and K_2CO_3 (4.0 equiv) were dissolved in acetone (10 mL). The solution was stirred at 60 °C for 12 h. After the reaction mixture was cooled and the solvent was removed by evaporators, the residue was treated with H_2O (15 mL) and extracted with EA. The combined organic layers were washed with water, dried over Na_2SO_4, and evaporated by vacuum. The crude product was purified using flash column chromatography to give compound **8b** (213 mg, 94%). ^{1}H NMR (300 MHz, $CDCl_3$): δ 7.03 (d, J = 8.4 Hz, 2H), δ 6.84 (d, J = 8.7 Hz, 2H), 6.11−5.98 (m, 1H), 5.40 (dd, J = 1.5 Hz, 1H), 5.27 (dd, J = 1.2 Hz, 1H), 4.94 (s, 1H), 4.51 (d, J = 5.4 Hz, 2H), 3.70 (s, 3H), 3.03 (t, J = 7.8 Hz, 2H), and 1.42 (s, 9H).

*Synthesis of O-Propargyl 1,2:3,4-Di-O-isopropylidene-D-galactopyranose (**9a**).* To a stirred solution of 1,2:3,4-di-*O*-isopropylidene-D-galactopyranose (100 mg) in DMF (10 mL) at 0 °C was carefully added NaH (60% in mineral oil, 30 mg). The reaction mixture was stirred for 30 min until hydrogen evolution stopped. Propargyl bromide (66 μL) was added, and the mixture was stirred at 0 °C for 30 min and then at room temperature for 12 h. Then the reaction mixture was poured into brine, and extracted with ether (150 mL × 3). The combined organic layers were washed with brine, dried over Na_2SO_4, and concentrated. The residue was purified by chromatography to give compound **9a** (84 mg, 73%). ^{1}H NMR (300 MHz, $CDCl_3$): δ 5.54 (d, J = 5.1 Hz, 1H), 4.60 (dd, J = 2.1, 2.4 Hz, 1H), 4.32−4.20 (m, 4H), 4.02−3.97 (m, 1H), 3.77 (q, J = 4.8 Hz, 1H), 3.67 (q, J = 3.0 Hz, 1H), 2.42 (t, J = 2.4 Hz, 1H), 1.54 (s, 3H), 1.45 (s, 3H), and 1.33 (d, J = 4.2 Hz, 6H).

*Synthesis of O-Allyl 1,2:3,4-Di-O-isopropylidene-D-galactopyranose (**9b**).* To a stirred solution of *O*-propargyl 1,2:3,4-di-*O*-isopropylidene-D-galactopyranose (100 mg) in DMF (10 mL) at 0 °C was carefully added NaH (60% in mineral oil, 30 mg). The reaction mixture was stirred for 30 min until hydrogen evolution stopped. Allyl bromide (67 μL) was added, and the mixture was stirred at 0 °C for 30 min and then at room temperature for 12 h. Then the reaction mixture was poured into brine, and extracted with ether (150 mL × 3). The combined organic layers were washed with brine, dried over Na_2SO_4, and concentrated. The residue was purified by chromatography to give compound **9b** (87 mg, 76%). ^{1}H NMR (300 MHz, $CDCl_3$): δ 5.98−5.85 (m, 1H), 5.53 (d, J = 5.1 Hz, 1H), 5.21 (q, J = 17.1 Hz, 2H), 4.60 (dd, J = 2.1 Hz, 1H), 4.32−4.25 (m, 2H), 4.04 (s, 2H), 3.98 (m, J = 6.0 Hz, 1H), 3.69−3.55 (m, 2H), 1.54 (s, 3H), 1.44 (s, 3H), and 1.33 (d, J = 3.6 Hz, 6H).

*Synthesis of 1-(N-Methylethanolamine-N-yl)-diazen-1-ium-1,2-diolate Sodium Salt (**11**).* To a solution of *N*-methylethanolamine (**10**, 10.0 g) in ether (150 mL) in a Teflon bottle was added a mixture of sodium methoxide (1.05 equiv) in methanol (20 mL). The bottle was sealed, flushed with nitrogen (five times), and charged with NO gas (50 psi). After 24 h, a white precipitate was collected by filtration and washed with copious amounts of ether to produce compound **11**, which was used without further purification.

*General Procedure for the Synthesis of Compounds **12** and **13**.* Compound **11** (1.0 g, 6.37 mmol) was suspended in 5 mL of DMF at 0 °C under a steady stream of nitrogen, to which was added propargyl bromide (757.78 mg, 6.37 mmol) or iodomethane (904.16 mg, 6.37 mmol). The reaction mixture was allowed to warm to room temperature and stirred overnight. Then the solvent was removed under vacuum, and the obtained residue was added into H_2O (20 mL) and extracted with EA (3 × 50 mL). The combined organic layers were washed with brine (20 mL), dried over Mg_2SO_4, and evaporated under vacuum. The crude product was purified by flash chromatography on silica gel by using EA and hexane for eluting to give target compounds **12**[26] and **13**.[59]

*O^2-Propargyl 1-(N-Methylethanolamine-N-yl)-diazen-1-ium-1,2-diolate (**12**).* Colorless oil, 562 mg, yield 51%. ^{1}H NMR (ppm, 300 MHz, $CDCl_3$): δ 4.77 (d, J = 2.4 Hz, 2H), 3.74 (t, J = 4.8 Hz, 2H), 3.42 (t, J = 4.8 Hz, 2H), 3.05 (s, 3H), 2.55 (t, J = 2.4 Hz, 1H), and 2.50 (br, 1H). ^{13}C NMR (ppm, 75 MHz, $CDCl_3$): δ 76.33, 60.97, 59.56, 57.05, and 41.90. MS (ESI) m/z: $C_6H_{11}N_3O_3$, $[M + Na]^+$ = 196.3.

*O^2-Methyl 1-(N-Methylethanolamine-N-yl)-diazen-1-ium-1,2-diolate (**13**).* Light yellow oil, 607 mg, yield 64%. ^{1}H NMR (ppm, 500 MHz, $CDCl_3$): δ 4.01 (s, 3H), 3.73 (t, J = 4.5 Hz, 2H), 3.38 (t, J = 5.0 Hz, 2H), 3.00 (s, 3H), and 2.32 (s, 1H). ^{13}C NMR (ppm, 75 MHz, $CDCl_3$): δ 60.64, 59.02, 56.74, and 41.68. ESI-MS m/z: $C_4H_{11}N_3O_3$, $[M + Na]^+$ = 172.1.

*General Procedure for the Synthesis of Compound **14** or **15**.* To a solution of **12** (700 mg, 4.05 mmol) or **13** (602 mg, 4.03 mmol) in anhydrous THF (10 mL) was added 4-dimethylaminopyridine (122 mg, 1.0 mmol), and the obtained mixture was allowed to stir at room temperature for 15 min. A solution of anhydrous THF (5 mL) containing succinic anhydride (608 mg, 6.08 mmol) was added dropwise to the reaction mixture, and the obtained mixture was allowed to reflux overnight. After the reaction, solid residues were removed by filtration, and the filtrate was concentrated under vacuum. Then, the resulting residue was added to H_2O (50 mL) and extracted with DCM (6 × 30 mL). The combined organic layers were washed with brine (20 mL), dried with Mg_2SO_4, filtrated, and evaporated to afford compounds **14** or **15** without further purification.

*O^2-Propargyl 1-(N-methyl-2-(4-oxo-butanoic acid-4-yl)-oxy-ethylamine-N-yl)-diazen-1-ium-1,2-diolate (**14**).* Light yellow oil, 863 mg, yield 78%. ^{1}H NMR (ppm, 300 MHz, $CDCl_3$): δ 4.78 (d, J = 2.1 Hz, 2H), 4.29 (t, J = 5.4 Hz, 2H), 3.60 (t, J = 5.4 Hz, 2H), 3.07 (s, 3H), 2.70−2.60 (m, 4H), and 2.55 (t, J = 2.4 Hz, 1H). ^{13}C NMR (ppm, 75 MHz, $CDCl_3$): δ 176.86, 171.40, 77.13, 75.76, 60.96, 60.43, 52.26, 40.92, and 28.30. ESI-MS m/z: 296.1, $[M + Na]^+$; HRMS (ESI): calcd for $C_{10}H_{15}N_3O_6$, $[M - H]^-$ 272.0888; found, 272.0897, ppm error 3.3.

*O^2-Methyl 1-(N-methyl-2-(4-oxo-butanoic acid-4-yl)-oxy-ethylamine-N-yl)-diazen-1-ium-1,2-diolate (**15**).* Light yellow oil, 725 mg, yield 72%. ^{1}H NMR (ppm, 500 MHz, $CDCl_3$): δ 4.26 (t, J = 5.5 Hz, 2H), 4.00 (s, 3H), 3.53 (t, J = 5.5 Hz, 2H), 3.01 (s, 3H), and 2.68−2.60 (m, 4H). ^{13}C NMR (ppm, 125 MHz, $CDCl_3$): δ 177.36, 177.83, 61.44, 61.02, 52.90, 41.76, and 28.74. ESI-MS m/z: 272.1, $[M + Na]^+$; HRMS (ESI): calcd for $C_8H_{15}N_3O_6$, $[M - H]^-$ 248.0888; found, 248.0892, ppm error 1.6.

*General Procedure for the Synthesis of Compound **16** or **17**.* To a mixture of **14** (217 mg, 0.79 mmol) or **15** (200 mg, 0.80 mmol) and Et_3N (86.6 mg, 0.86 mmol) in anhydrous DMF (5 mL) was added 2-(1H-benzotriazole-1-yl)-1,1,3,3-tetramethyluronium tetrafluoroborate (TBTU, 265 mg, 0.83 mmol), and the reaction mixture was stirred at room temperature for 30 min. Then diamine trichloro hydroxy platinum (**3**) (200 mg, 0.57 mmol) was added, and the mixture was stirred in the dark for 12 h. The reaction mixture was distilled under vacuum to remove DMF. The obtained residue was purified by silica gel chromatography by using DCM and methanol for eluting to obtain the final products **16** and **17**.

*O^2-Propargyl 1-(N-Methyl-2-(4-oxo-butanoic acid diamine trichloro hydroxyl platinum ester-4-yl)-oxy-ethylamine-N-yl)-diazen-1-ium-1,2-diolate (**16**).* Light yellow solid, 84 °C (decomposition), 97 mg, yield 28%. ^{1}H NMR (ppm, 300 MHz, DMSO-d_6): δ 6.28−6.03 (m, 6H), 4.82 (d, J = 2.4 Hz, 2H), 4.16 (t, J = 5.4 Hz, 2H), 3.58 (t, J = 2.4 Hz, 2H), 2.98 (s, 3H), and 2.49−2.42 (m, 5H). ^{13}C NMR (ppm, 75 MHz, DMSO-d_6): δ 178.90, 172.01, 78.75, 60.54, 60.39, 51.83, 40.52, 30.94, and 29.80. HRMS (ESI): calcd for $C_{10}H_{20}Cl_3N_5O_6Pt$, $[M + H]^+$ 607.0200; found, 607.0191, ppm error −1.5.

*O^2-Methyl 1-(N-Methyl-2-(4-oxo-butanoic acid diamine trichloro hydroxyl platinum ester-4-yl)-oxy-ethylamine-N-yl)-diazen-1-ium-1,2-diolate (**17**).* Light yellow solid, 103 °C (decomposition), 134 mg, yield 37.4%. ^{1}H NMR (ppm, 500 MHz, DMSO-d_6): δ 6.28−6.03 (m,

https://dx.doi.org/10.1021/acs.jmedchem.0c01435
J. Med. Chem. XXXX, XXX, XXX−XXX

6H), 4.15 (t, J = 5.0 Hz, 2H), 3.90 (s, 3H), 3.52 (t, J = 5.0 Hz, 2H), 2.95 (s, 3H), and 2.52−2.44 (m, 4H). ^{13}C NMR (ppm, 125 MHz, DMSO-d_6): δ 182.01, 175.12, 63.69, 63.57, 55.06, 43.86, 34.06, and 32.93. HRMS (ESI): calcd for $C_8H_{20}Cl_3N_5O_6Pt$, $[M + H]^+$ 583.0200; found, 583.0191, ppm error −1.5.

Synthesis of RDC1. RDC1 was synthesized from 7-(diethylamino)-coumarin-3-carboxylic acid and Rho-6G as per previously reported procedures.[46] ^{1}H NMR (300 MHz, $CDCl_3$): δ 7.89 (d, J = 8.5 Hz, 2H), 7.33 (t, J = 9.0 Hz, 3H), 6.98 (d, J = 7.2 Hz, 1H), 6.67−6.53 (m, 3H), 6.49 (s, 1H), 6.33 (s, 2H), 4.49 (t, J = 6.1 Hz, 2H), 4.25 (s, 4H), 3.80 (d, J = 6.2 Hz, 4H), 3.44 (q, J = 7.2 Hz, 6H), 3.20 (q, J = 7.2 Hz, 4H), 1.96 (s, 6H), and 1.32−1.25 (m, 12H). ESI-MS m/z: 877.5, $[M + H]^+$.

Decaging of Compound ***5a***. A solution of the compounds **5a** (500 μM) and **1** (500 μM) in PBS (5 mL, pH 7.4) containing 5% DMSO was incubated at 37 °C. An aliquot (400 μL) at 24 h was subjected to HPLC analysis to determine the concentration of generating **5** according to the previously established standard curve of concentrations-peak areas. The conversion ratio from **5a** to **5** was 76%.

Decaging of Compound ***5b***. A solution of the compounds **5b** (500 μM) and **1** (500 μM) in PBS (5 mL, pH 7.4) containing 5% DMSO was incubated at 37 °C. An aliquot (400 μL) at 24 h was subjected to HPLC analysis to determine the concentration of generating **5** according to the previously established standard curve of concentration-peak areas. The conversion ratio from **5b** to **5** was 13%.

Decaging of Compound ***5c***. A solution of the compounds **5c** (500 μM) and **1** (500 μM) in PBS (5 mL, pH 7.4) containing 5% DMSO was incubated at 37 °C. An aliquot (400 μL) at 24 h was subjected to HPLC analysis to determine the concentration of generating **5** according to the previously established standard curve of concentration-peak areas. The conversion ratio from **5c** to **5** was 12%.

Decaging of Compound ***5d***. A solution of compounds **5d** (500 μM) and **1** (500 μM) in PBS (5 mL, pH 7.4) containing 5% DMSO was incubated at 37 °C. An aliquot (400 μL) at 24 h was subjected to HPLC analysis to determine the concentrations of generating **5** according to the previously established standard curve of concentration-peak areas. The conversion ratio from **5d** to **5** was 79%.

Decaging of Compound ***6a***. A solution of compounds **6a** (125 μM) and **1** (125 μM) in PBS (5 mL, pH 7.4) containing 5% DMSO was incubated at 37 °C. At 24 h, the concentration of NO (presented as NO_2^-) was measured by using nitrite colorimetric kit. The conversion ratio from **6a** to NO was 41%.

Decaging of Compound ***6b***. A solution of compounds **6b** (125 μM) and **1** (125 μM) in PBS (5 mL, pH 7.4) containing 5% DMSO was incubated at 37 °C. At 24 h, the concentration of NO (presented as NO_2^-) was measured by using nitrite colorimetric kit. The conversion ratio from **6b** to NO was 8.7%.

Decaging of Compound ***7a***. A solution of compounds **7a** (500 μM) and **1** (500 μM) in PBS (5 mL, pH 7.4) containing 5% DMSO were incubated at 37 °C. An aliquot (400 μL) at 24 h was subjected to HPLC analysis to determine the concentration of generating **7** according to the previously established standard curve of concentration-peak areas. The conversion ratio from **7a** to **7** was 66%.

Decaging of Compound ***7b***. A solution of compounds **7b** (500 μM) and **1** (500 μM) in PBS (5 mL, pH 7.4) containing 5% DMSO was incubated at 37 °C. An aliquot (400 μL) at 24 h was subjected to HPLC analysis to determine the concentration of generating **7** according to the previously established standard curve of concentration-peak areas. The conversion ratio from **7b** to **7** was 92%.

Decaging of Compound ***8a***. A solution of compounds **8a** (500 μM) and **1** (500 μM) in PBS (5 mL, pH 7.4) containing 5% DMSO was incubated at 37 °C. An aliquot (400 μL) at 24 h was subjected to HPLC analysis to determine the concentration of generating **8** according to the previously established standard curve of concentration-peak areas. The conversion ratio from **8a** to **8** was 18%.

Decaging of Compound ***8b***. A solution of compounds **8b** (500 μM) and **1** (500 μM) in PBS (5 mL, pH 7.4) containing 5% DMSO was incubated at 37 °C. An aliquot (400 μL) at 24 h was subjected to HPLC analysis to determine the concentration of generating **8** according to the previously established standard curve of concentrations-peak areas. The conversion ratio from **8b** to **8** was 13%.

Decaging of Compound ***9a***. Compound **9a** (29.8 mg) and **1** (30.0 mg) were stirred in PBS (10 mL, pH 7.4) containing 5% DMSO and 5% DMF at 37 °C for 48 h. After the reaction mixture was cooled and the solvent was removed by evaporators, the residue was purified by flash chromatography to afford compound **9** (7.54 mg, 29%). ^{1}H NMR (300 MHz, $CDCl_3$): δ 5.57 (d, J = 5.1 Hz, 1H), 4.61 (dd, J = 2.1, 2.4 Hz, 1H), 4.34−4.26 (m, 2H), 3.85 (t, J = 7.5 Hz, 2H), 3.75 (q, J = 6.6 Hz, 1H), 1.53 (s, 3H), 1.45 (s, 3H), and 1.33 (s, 6H).

Decaging of Compound ***9b***. Compound **9b** (30.0 mg) and **1** (30.0 mg) were stirred in PBS (10 mL, pH 7.4) containing 5% DMSO and 5% DMF at 37 °C for 48 h. After the reaction mixture was cooled and the solvent was removed by evaporators, the residue was purified by flash chromatography to afford compound **9** (4.68 mg, 18%).

MTT Assay. Human ovarian cancer A2780 cells and human normal ovarian epithelial IOSE80 cells were purchased from American type culture collection. The cells were planked in a 96-well plate with a concentration of 10^4 cells/well and cultured in 37 °C under 5% CO_2 until 90% cells fused. Then the cells were incubated in serum-free RPMI 1640 or McCoy's 5A culture medium for 2 h for synchronization. Subsequently, the supernatant was discarded, and RPMI 1640 or McCoy's 5A medium with or without different concentrations of **3** were added and incubated for 10 h. After incubation, the supernatant was discarded and cells were rinsed with PBS three times. Then cells were treated with test compounds for 72 h. Four hours before the end of incubation, MTT solution (5 mg/mL, 20 μL) was added to each well. After incubation for 4 h, the supernatant of each well was discarded and 150 μL of DMSO was added. The cells were oscillated for 10 min in a cell oscillation apparatus, and OD_{570} was determined by enzyme labeling after the crystal was fully dissolved. The cell viability was expressed as a percentage of OD_{570}. IC_{50} values were calculated by GraphPad Prism 6.0.

Measurement of NO-Release Behavior of Related Compounds in Living Cells. For groups of **14** and **15**, A2780 or IOSE80 cells in 96-well plates were treated without or with **3** for 10 h, followed by being rinsed with PBS three times. Subsequently, the cells were resuspended with equivalent concentration of test compounds (**14** or **15**) for additional 8 h. While for other groups, A2780 or IOSE80 cells in 96-well plates were treated with the test compounds at indicated concentrations for indicated times. The cells were then collected and resuspended with DAF-FM DA (1.5 mL, 5 μM) at 37 °C for 20 min in the dark. The cells were rinsed three times with PBS and then analyzed by FACS. NO production was measured with the flow cytometer with excitation and emission wavelengths of 495 and 515 nm, respectively. BD Accuri C6 flow cytometer was used, and 10,000 cells was gated for each sample.

Cellular Accumulation of Platinum. The cellular accumulation of platinum was investigated as per the reported method. A2780 or IOSE80 cells (2.5×10^6) were seeded in 75 cm^2 flasks in growth medium (20 mL). After overnight incubation, the medium was replaced and the cells were treated with **16** or **1** at the concentration of 5 μM for 24 h. Cell monolayers were washed twice with cold PBS, harvested, and counted. Cell nuclei were isolated by means of the nuclei isolation kit Nuclei EZ Prep (Sigma-Aldrich, St. Louis, MO). Then samples were subjected to three freezing/thawing cycles at −80 °C and then vigorously vortexed. The samples were treated with highly pure nitric acid (Pt: ≤0.01 μg kg^{-1}, Sigma Chemical, St. Louis, MO) and transferred into a microwave Teflon vessel. Subsequently, samples were submitted to standard procedures using a speed wave MWS-3 Berghof instrument (Eningen, Germany). After cooling, each mineralized sample was analyzed for platinum by using a Varian AA Duo graphite furnace atomic absorption spectrometer (Varian, Palo Alto, CA; USA) at the wavelength of 324.7 nm.

Measurement of Water−Octanol Partition Coefficient (Log*Po*/w) for 16. We used the shake flask method to determine the partition coefficient (P) of **16**. Octanol was saturated with a PBS buffer by shaking the two-phase mixture overnight. And then 50 μM **16** was added to a mixture of octanol-saturated water (5 mL) and water-saturated octanol (5 mL) in a 15 mL tube. The tube was shaken at room temperature in the dark for 6 h. The two phases were separated by centrifugation, and the **16** concentrations in these two phases were

https://dx.doi.org/10.1021/acs.jmedchem.0c01435
J. Med. Chem. XXXX, XXX, XXX−XXX

determined by HPLC. The LogPo/w was expressed as a mean of three independent experiments.

DNA Platination. A2780 or IOSE80 cells (3×10^6) were seeded in 10 cm Petri dishes in 10 mL of culture medium. Subsequently, cells were treated with **16** or **1** at the concentration of 5 μM for 24 h. DNA was extracted and purified by a commercial spin column quantification kit (Qiagen, Valencia, CA). Only highly purified samples (A260/A230 $\cong$ 1.8 and A280/A260 $\cong$ 2.0) were included for analysis to avoid any artifacts. The samples were completely dried and redissolved in 200 μL of Milli-Q water (18.2 MΩ) for at least 20 min at 65 °C in a shaking thermo-mixer, mineralized and analyzed for total Pt content by GF-AAS as described above.

Establishment of Zebrafish Embryo Ovarian Cancer Model. First, the ovarian cancer cells A2780 were collected in DMEM (with 10% fetal bovine serum), then A2780 and 10 μg/mL CM-DiI solution (5% DMSO/water) and were incubated together until fluorescence was observed (~15 min), and the cell density was adjusted to 2×10^7 cells/mL. The labeled cells were microinjected into the yolk space of 2 dpf zebrafish juveniles within 2 h. The number of cells was controlled to about 400 per fish. The zebrafish were cultivated at 37 °C for 24 h; totally 40−60 fish with successful transplantation were selected under fluorescence microscopy for further assays. All animal experiments and animal care were conducted in accordance with the guidelines of the Provision and General Recommendation of Chinese Experimental Animals in China. The experimental protocols were approved by the Animal Research and Care Committee of China Pharmaceutical University [SYXK (SU) 2016-0011].

■ ASSOCIATED CONTENT

Supporting Information

The Supporting Information is available free of charge at https://pubs.acs.org/doi/10.1021/acs.jmedchem.0c01435.

The depropargylation efficacy catalyzed by various Pt complexes (Figures S1 and S2), the degradation of compound **6a** and NO release from **6a** in the presence of **1** or **3** (Figure S3), **1**-mediated cleavage reactions of various substrates (Table S1), the effects of temperatures, water, and pH values on the **1**-triggered depropargylation (Figure S4), the LC−MS spectrum of the reaction mixture of **1** with **5a** (Figure S5), the decomposition kinetics of **14** and **15** in different conditions measured by HPLC (Figure S6), NO released from the test compounds in A2780 and IOSE80 cells (Figure S7), the representative confocal microscopy images of established zebrafish models (Figure S8), ^{1}H NMR, ^{13}C NMR, HRMS, and HPLC spectra for compounds **14**−**17** (PDF)

Molecular formula strings for target compounds **14**−**17** and the calculated IC_{50} values against A2780 and IOSE80 cells (CSV)

■ AUTHOR INFORMATION

Corresponding Author

Zhangjian Huang − *State Key Laboratory of Natural Medicines, Jiangsu Key Laboratory of Drug Discovery for Metabolic Diseases, Jiangsu Key Laboratory of Drug Screening, China Pharmaceutical University, Nanjing 210009, P. R. China;* orcid.org/0000-0001-6409-8535; Email: zhangjianhuang@cpu.edu.cn

Authors

Tao Sun − *State Key Laboratory of Natural Medicines, Jiangsu Key Laboratory of Drug Discovery for Metabolic Diseases, Jiangsu Key Laboratory of Drug Screening, China Pharmaceutical University, Nanjing 210009, P. R. China*

Tian Lv − *State Key Laboratory of Natural Medicines, Jiangsu Key Laboratory of Drug Discovery for Metabolic Diseases, Jiangsu Key Laboratory of Drug Screening, China Pharmaceutical University, Nanjing 210009, P. R. China*

Jianbing Wu − *State Key Laboratory of Natural Medicines, Jiangsu Key Laboratory of Drug Discovery for Metabolic Diseases, Jiangsu Key Laboratory of Drug Screening, China Pharmaceutical University, Nanjing 210009, P. R. China;* orcid.org/0000-0003-2725-9859

Mingchao Zhu − *State Key Laboratory of Natural Medicines, Jiangsu Key Laboratory of Drug Discovery for Metabolic Diseases, Jiangsu Key Laboratory of Drug Screening, China Pharmaceutical University, Nanjing 210009, P. R. China*

Yue Fei − *State Key Laboratory of Natural Medicines, Jiangsu Key Laboratory of Drug Discovery for Metabolic Diseases, Jiangsu Key Laboratory of Drug Screening, China Pharmaceutical University, Nanjing 210009, P. R. China*

Jie Zhu − *State Key Laboratory of Natural Medicines, Jiangsu Key Laboratory of Drug Discovery for Metabolic Diseases, Jiangsu Key Laboratory of Drug Screening, China Pharmaceutical University, Nanjing 210009, P. R. China*

Yihua Zhang − *State Key Laboratory of Natural Medicines, Jiangsu Key Laboratory of Drug Discovery for Metabolic Diseases, Jiangsu Key Laboratory of Drug Screening, China Pharmaceutical University, Nanjing 210009, P. R. China;* orcid.org/0000-0003-2378-7064

Complete contact information is available at: https://pubs.acs.org/10.1021/acs.jmedchem.0c01435

Author Contributions

†T.S., T.L., and J.W. contributed equally to this work.

Notes

The authors declare no competing financial interest.

■ ACKNOWLEDGMENTS

This work was supported by the National Natural Science Foundation of China (nos. 81822041, 21977116, 81673305 and 81773573), National Science & Technology Major Project "Key New Drug Creation and Manufacturing Program" (number: 2018ZX09711002-006-013), the Funding of Double First-Rate Discipline Construction (CPU2018GY06 and CPU2018GY18), open project of State Key Laboratory of Natural Medicines, nos. SKLNMZZCX201824 and SKLNMZZ202029, and State Key Laboratory of Pathogenesis, Prevention and Treatment of High Incidence Diseases in Central Asia Fund (SKL-HIDCA-2018-1). We also thank Nanjing Xinjia Medical Technology Corporation for assistance with the zebrafish assays. The authors thank Dr. Binghe Wang from Georgia State University for manuscript editing.

■ ABBREVIATIONS

NO, nitric oxide; PTIO, 2-phenyl-4,4,5,5-tetramethylimidazoline-1-oxyl 3-oxide; DAF-FM DA, 4-amino-5-(methylamino)-2′,7′-difluoro-fluorescein diacetate; PBS, phosphate buffered solution; NCS, *N*-chlorosuccinimide; EA, ethyl acetate; FACS, fluorescence-activated cell sorting; TBTU, 2-(1H-benzotriazole-1-yl)-1,1,3,3-tetramethyluronium tetrafluoroborate; DMF, *N*,*N*-dimethylformamide; DMAP, 4-dimethylaminopyridine

■ REFERENCES

(1) Saxon, E.; Bertozzi, C. R. Cell Surface Engineering by a Modified Staudinger Reaction. *Science* **2000**, *287*, 2007−2010.

(2) Kolb, H. C.; Finn, M. G.; Sharpless, K. B. Click Chemistry: Diverse Chemical Function From a Few Good Reactions. *Angew. Chem., Int. Ed.* **2001**, *40*, 2004−2021.
(3) Prescher, J. A.; Dube, D. H.; Bertozzi, C. R. Chemical Remodelling of Cell Surfaces in Living Animals. *Nature* **2004**, *430*, 873−877.
(4) Prescher, J. A.; Bertozzi, C. R. Chemistry in Living Systems. *Nat. Chem. Biol.* **2005**, *1*, 13−21.
(5) Bertozzi, C. R. Decade of Bioorthogonal Chemistry. *Acc. Chem. Res.* **2011**, *44*, 651−653.
(6) Wang, J.; Cheng, B.; Li, J.; Zhang, Z.; Hong, W.; Chen, X.; Chen, P. R. Chemical Remodeling of Cell-Surface Sialic Acids Through a Palladium-Triggered Bioorthogonal Elimination Reaction. *Angew. Chem., Int. Ed.* **2015**, *54*, 5364−5368.
(7) Li, J.; Chen, P. R. Development and Application of Bond Cleavage Reactions in Bioorthogonal Chemistry. *Nat. Chem. Biol.* **2016**, *12*, 129−137.
(8) Wang, J.; Liu, Y.; Liu, Y.; Zheng, S.; Wang, X.; Zhao, J.; Yang, F.; Zhang, G.; Wang, C.; Chen, P. R. Time-resolved Protein Activation by Proximal Decaging in Living Systems. *Nature* **2019**, *569*, 509−513.
(9) Li, J.; Yu, J.; Zhao, J.; Wang, J.; Zheng, S.; Lin, S.; Chen, L.; Yang, M.; Jia, S.; Zhang, X.; Chen, P. R. Palladium-triggered Deprotection Chemistry for Protein Activation in Living Cells. *Nat. Chem.* **2014**, *6*, 352−361.
(10) Pérez-López, A. M.; Rubio-Ruiz, B.; Sebastián, V.; Hamilton, L.; Adam, C.; Bray, T. L.; Irusta, S.; Brennan, P. M.; Lloyd-Jones, G. C.; Sieger, D.; Santamaría, J.; Unciti-Broceta, A. Gold-Triggered Uncaging Chemistry in Living Systems. *Angew. Chem., Int. Ed.* **2017**, *56*, 12548−12552.
(11) Weiss, J. T.; Dawson, J. C.; Macleod, K. G.; Rybski, W.; Fraser, C.; Torres-Sanchez, C.; Patton, E. E.; Bradley, M.; Carragher, N. O.; Unciti- Broceta, A. Extracellular Palladium-Catalysed Dealkylation of 5-fluoro-1-propargyl-uracil as a Bioorthogonally Activated Prodrug Approach. *Nat. Commun.* **2014**, *5*, 3277−3285.
(12) Wang, J.; Zheng, S.; Liu, Y.; Zhang, Z.; Lin, Z.; Li, J.; Zhang, G.; Wang, X.; Li, J.; Chen, P. R. Palladium-Triggered Chemical Rescue of Intracellular Proteins via Genetically Encoded Allene-Caged Tyrosine. *J. Am. Chem. Soc.* **2016**, *138*, 15118−15121.
(13) Streu, C.; Meggers, E. Ruthenium-induced Allylcarbamate Cleavage in Living Cells. *Angew. Chem., Int. Ed.* **2006**, *25*, 5645−5648.
(14) Fan, X.; Ge, Y.; Lin, F.; Yang, Y.; Zhang, G.; Ngai, W. S. C.; Lin, Z.; Zheng, S.; Wang, J.; Zhao, J.; Li, J.; Chen, P. R. Optimized Tetrazine Derivatives for Rapid Bioorthogonal Decaging in Living Cells. *Angew. Chem., Int. Ed.* **2016**, *55*, 14046−14050.
(15) Tu, J.; Xu, M.; Parvez, S.; Peterson, R. T.; Franzini, R. M. Bioorthogonal Removal of 3-Isocyanopropyl Groups Enables the Controlled Release of Fluorophores and Drugs in vivo. *J. Am. Chem. Soc.* **2018**, *140*, 8410−8414.
(16) Versteegen, R. M.; Rossin, R.; ten Hoeve, W.; Janssen, H. M.; Robillard, M. S. Click to Release: Instantaneous Doxorubicin Elimination Upon Tetrazine Ligation. *Angew. Chem., Int. Ed.* **2013**, *52*, 14112−14116.
(17) Matikonda, S. S.; Orsi, D. L.; Staudacher, V.; Jenkins, I. A.; Fiedler, F.; Chen, J.; Gamble, A. B. Bioorthogonal Prodrug Activation Driven by a Strain-Promoted 1,3-dipolar Cycloaddition. *Chem. Sci.* **2015**, *6*, 1212−1218.
(18) Zheng, Y.; Ji, X.; Yu, B.; Ji, K.; Gallo, D.; Csizmadia, E.; Zhu, M.; Choudhury, M. R.; De La Cruz, L. K. C.; Chittavong, V.; Pan, Z.; Yuan, Z.; Otterbein, L. E.; Wang, B. Enrichment-triggered Prodrug Activation Demonstrated Through Mitochondria-Targeted Delivery of Doxorubicin and Carbon Monoxide. *Nat. Chem.* **2018**, *10*, 787−794.
(19) Oliveira, B. L.; Stenton, B. J.; Unnikrishnan, V. B.; de Almeida, C. R.; Conde, J.; Negrão, M.; Schneider, F. S. S.; Cordeiro, C.; Ferreira, M. G.; Caramori, G. F.; Domingos, J. B.; Fior, R.; Bernardes, G. J. L. Platinum-triggered Bond-cleavage of Pentynoyl amide and N-propargyl Handles for Drug-Activation. *J. Am. Chem. Soc.* **2020**, *142*, 10869−10880.
(20) Rubio-Ruiz, B.; Weiss, J. T.; Unciti-Broceta, A. Efficient Palladium-Triggered Release of Vorinostat From a Bioorthogonal Precursor. *J. Med. Chem.* **2016**, *59*, 9974−9980.
(21) Stenton, B. J.; Oliveira, B. L.; Matos, M. J.; Sinatra, L.; Bernardes, G. J. L. A Thioether-Directed Palladium-Cleavable Linker for Targeted Bioorthogonal Drug Decaging. *Chem. Sci.* **2018**, *9*, 4185−4189.
(22) Li, B.; Liu, P.; Wu, H.; Xie, X.; Chen, Z.; Zeng, F.; Wu, S. A Bioorthogonal Nanosystem for Imaging and in Vivo Tumor Inhibition. *Biomaterials* **2017**, *138*, 57−68.
(23) Yao, Q.; Lin, F.; Fan, X.; Wang, Y.; Liu, Y.; Liu, Z.; Jiang, X.; Chen, P. R.; Gao, Y. Synergistic Enzymatic and Bioorthogonal Reactions for Selective Prodrug Activation in Living Systems. *Nat. Commun.* **2018**, *9*, 1−9.
(24) Sancho-Albero, M.; Rubio-Ruiz, B.; Pérez-López, A. M.; Sebastián, V.; Martín-Duque, P.; Arruebo, M.; Santamaría, J.; Unciti-Broceta, A. Cancer-derived Exosomes Loaded With Ultrathin Palladium Nanosheets for Targeted Bioorthogonal Catalysis. *Nat. Catal.* **2019**, *2*, 864−872.
(25) Konter, J.; Abuo-Rahma, G. E.-D. A. A.; El-Emam, A.; Lehmann, J. Synthesis of Diazen-1-ium-1,2-diolates Monitored by the "NO tizer" Apparatus: Relationship between Formation Rates, Molecular Structure and the Release of Nitric Oxide. *Eur. J. Org. Chem.* **2007**, *2007*, 616−624.
(26) Lv, T.; Wu, J.; Kang, F.; Wang, T.; Wan, B.; Lu, J.-J.; Zhang, Y.; Huang, Z. Synthesis and Evaluation of O^2- Derived Diazeniumdiolates Activatable via Bioorthogonal Chemistry Reactions in Living Cells. *Org. Lett.* **2018**, *20*, 2164−2167.
(27) Johnstone, T. C.; Suntharalingam, K.; Lippard, S. J. The Next Generation of Platinum Drugs: Targeted Pt(II) Agents, Nanoparticle Delivery, and Pt(IV) Prodrugs. *Chem. Rev.* **2016**, *116*, 3436−3486.
(28) Awuah, S. G.; Zheng, Y.-R.; Bruno, P. M.; Hemann, M. T.; Lippard, S. J. A Pt(IV) Pro-drug Preferentially Targets Indoleamine-2,3-dioxygenase, Providing Enhanced Ovarian Cancer Immuno-Chemotherapy. *J. Am. Chem. Soc.* **2015**, *137*, 14854−14857.
(29) Wang, X.; Guo, Z. Targeting and Delivery of Platinum-Based Anticancer Drugs. *Chem. Soc. Rev.* **2013**, *42*, 202−224.
(30) Wang, Z.; Xu, Z.; Zhu, G. A Platinum(IV) Anticancer Prodrug Targeting Nucleotide Excision Repair To Overcome Cisplatin Resistance. *Angew. Chem., Int. Ed.* **2016**, *55*, 15564−15568.
(31) Zhu, G.; Myint, M.; Ang, W. H.; Song, L.; Lippard, S. J. Monofunctional platinum-DNA Adducts Are Strong Inhibitors of Transcription and Substrates for Nucleotide Excision Repair in Live Mammalian Cells. *Cancer Res.* **2012**, *72*, 790−800.
(32) Gibson, D. Multi-action Pt(IV) Anticancer Agents; Do We Understand How They Work? *J. Inorg. Biochem.* **2019**, *191*, 77−84.
(33) Hall, M. D.; Hambley, T. W. Platinum(IV) Antitumour Compounds: Their Bioinorganic Chemistry. *Coord. Chem. Rev.* **2002**, *232*, 49−67.
(34) Weaver, E. L.; Bose, R. N. Platinum(II) Catalysis and Radical Intervention in Reductions of platinum(IV) Antitumor Drugs by Ascorbic Acid. *J. Inorg. Biochem.* **2003**, *95*, 231−239.
(35) Hrabie, J. A.; Keefer, L. K. Chemistry of the Nitric Oxide-Releasing Diazeniumdiolate ("Nitrosohydroxylamine") Functional Group and Its Oxygen-Substituted Derivatives. *Chem. Rev.* **2002**, *102*, 1135−1154.
(36) Carpenter, A. W.; Schoenfisch, M. H. Nitric Oxide Release: Part II. Therapeutic Applications. *Chem. Soc. Rev.* **2012**, *41*, 3742−3752.
(37) Huang, Z.; Fu, J.; Zhang, Y. Nitric Oxide Donor-Based Cancer Therapy: Advances and Prospects. *J. Med. Chem.* **2017**, *60*, 7617−7635.
(38) Chakrapani, H.; Showalter, B. M.; Citro, M. L.; Keefer, L. K.; Saavedra, J. E. Nitric Oxide Prodrugs: Diazeniumdiolate Anions of Hindered Secondary Amines. *Org. Lett.* **2007**, *9*, 4551−4554.
(39) Wink, D. A.; Cook, J. A.; Christodoulou, D.; Krishna, M. C.; Pacelli, R.; Kim, S.; DeGraff, W.; Gamson, J.; Vodovotz, Y.; Russo, A.; Mitchell, J. B. Nitric Oxide and Some Nitric Oxide Donor Compounds Enhance the Cytotoxicity of Cisplatin. *Nitric Oxide* **1997**, *1*, 88−94.
(40) Azizzadeh, B.; Yip, H. T.; Blackwell, K. E.; Horvath, S.; Calcaterra, T. C.; Buga, G. M.; Ignarro, L. J.; Wang, M. B. Nitric Oxide Improves Cisplatin Cytotoxicity in Head and Neck Squamous Cell Carcinoma. *Laryngoscope* **2001**, *111*, 1896−1900.

https://dx.doi.org/10.1021/acs.jmedchem.0c01435
J. Med. Chem. XXXX, XXX, XXX−XXX

(41) Zhao, J.; Gou, S.; Sun, Y.; Yin, R.; Wang, Z. Nitric Oxide Donor-Based Platinum Complexes as Potential Anticancer Agents. *Chem.—Eur. J.* **2012**, *18*, 14276−14281.
(42) Bredt, D. S.; Snyder, S. H. Nitric Oxide: A Physiologic Messenger Molecule. *Annu. Rev. Biochem.* **1994**, *63*, 175−195.
(43) Kojima, H.; Urano, Y.; Kikuchi, K.; Higuchi, T.; Hirata, Y.; Nagano, T. Fluorescent Indicators for Imaging Nitric Oxide Production. *Angew. Chem., Int. Ed.* **1999**, *38*, 3209−3212.
(44) Shami, P. J.; Saavedra, J. E.; Wang, L. Y.; Bonifant, C. L.; Diwan, B. A.; Singh, S. V.; Gu, Y.; Fox, S. D.; Buzard, G. S.; Citro, M. L.; Waterhouse, D. J.; Davies, K. M.; Ji, L. K. JS-K a Glutathione/Glutathione S-transferase-activated Nitric Oxide Donor of the Diazeniumdiolate Class With Potent Antineoplastic Activity. *Mol. Cancer Ther.* **2003**, *2*, 409−417.
(45) Huang, Z.; Wu, J.; Zou, Y.; Yuan, H.; Zhang, Y.; Fei, Y.; Bhardwaj, A.; Kaur, J.; Knaus, E. E.; Zhang, Y. Glutathione S-Transferase π-Activatable O^2-(Sulfonylethyl Derived) Diazeniumdiolates Potently Suppress Melanoma in vitro and in vivo. *J. Med. Chem.* **2018**, *61*, 1833−1844.
(46) Ong, J. X.; Lim, C. S. Q.; Le, H. V.; Ang, W. H. A Ratiometric Fluorescent Probe for Cisplatin: Investigating the Intracellular Reduction of Platinum(IV) Prodrug Complexes. *Angew. Chem., Int. Ed.* **2019**, *58*, 164−167.
(47) Raveendran, R.; Braude, J. P.; Wexselblatt, E.; Novohradsky, V.; Stuchlikova, O.; Brabec, V.; Gandin, V.; Gibson, D. Pt(IV) Derivatives of Cisplatin and Oxaliplatin With Phenylbutyrate Axial Ligands Are Potent Cytotoxic Agents That Act by Several Mechanisms of Action. *Chem. Sci.* **2016**, *7*, 2381−2391.
(48) Goncalves, A.; Domínguez, J. R.; Alvarado, J. Determination of Pd, Pt and Rh in Vehicles Escape Fumes by GF-AAS and ICP-OES. *Talanta* **2008**, *75*, 523−527.
(49) Kapp, T.; Dullin, A.; Gust, R. Platinum(II)-dendrimer Conjugates: Synthesis and Investigations on Cytotoxicity, Cellular Distribution, Platinum Release, DNA, and Protein Binding. *Bioconjugate Chem.* **2010**, *21*, 328−337.
(50) Aalbersberg, E. A.; van der Veen, B. J. d. W.; Zwaagstra, O.; van der Schilden, K. C.; Vegt, E.; Vogel, W. V. Preclinical Imaging Characteristics and Quantification of Platinum-195m SPECT. *Eur. J. Nucl. Med. Mol. Imag.* **2017**, *44*, 1347−1354.
(51) Novohradsky, V.; Zerzankova, L.; Stepankova, J.; Vrana, O.; Raveendran, R.; Gibson, D.; Kasparkova, J.; Brabec, V. New Insights Into the Molecular and Epigenetic Effects of Antitumor Pt(IV)-valproic Acid Conjugates in Human Ovarian Cancer Cells. *Biochem. Pharmacol.* **2015**, *95*, 133−144.
(52) Tu, J.; Svatunek, D.; Parvez, S.; Eckvahl, H. J.; Xu, M.; Peterson, R. T.; Houk, K. N.; Franzini, R. M. Isonitrile-responsive and Bioorthogonally Removable Tetrazine Protecting Groups. *Chem. Sci.* **2020**, *11*, 169−179.
(53) Dumitrescu, E.; Wallace, K. N.; Andreescu, S. Real Time Electrochemical Investigation of the Release, Distribution and Modulation of Nitric Oxide in the Intestine of Individual Zebrafish Embryos. *Nitric Oxide* **2018**, *74*, 32−38.
(54) Zhu, X.-Y.; Guo, D. W.; Lao, Q. C.; Xu, Y. Q.; Meng, Z. K.; Xia, B.; Yang, H.; Li, C. Q.; Li, P. Sensitization and Synergistic Anti-Cancer Effects of Furanodiene Identified in Zebrafish Models. *Sci. Rep.* **2019**, *9*, 4541.
(55) Wu, Q.; Zheng, K.; Huang, X.; Li, L.; Mei, W. Tanshinone-IIA-Based Analogues of Imidazole Alkaloid Act as Potent Inhibitors To Block Breast Cancer Invasion and Metastasis in vivo. *J. Med. Chem.* **2018**, *61*, 10488−10501.
(56) Stewart, J. F.; Tattersall, M. H. N.; Woods, R. L.; Fox, R. M. Cis-dichlorodiammine Platinum (II) in Advanced Ovarian Carcinoma. *Med. J. Aust.* **1979**, *1*, 548−550.
(57) Ravera, M.; Gabano, E.; Pelosi, G.; Fregonese, F.; Tinello, S.; Osella, D. A New Entry to Asymmetric platinum(IV) Complexes via Oxidative Chlorination. *Inorg. Chem.* **2014**, *53*, 9326−9335.
(58) Qin, X.; Fang, L.; Chen, F.; Gou, S. Conjugation of platinum(IV) Complexes With Chlorambucil to Overcome Cisplatin Resistance via a "Joint Action" Mode Toward DNA. *Eur. J. Med. Chem.* **2017**, *137*, 167−175.
(59) Smirnov, G. A.; Gordeev, P. B.; Nikitin, S. V.; Pokhvisneva, G. V.; Ternikova, T. V.; Luk'yanov, O. A. Synthesis of 1-Alkoxy-3-methyl-1-triazene 2-Oxides and 3, 3′-Methylene-bis(1-alkoxy-3-methyl-1-triazene 2-oxides). *Russ. Chem. Bull.* **2015**, *64*, 2712−2717.

https://dx.doi.org/10.1021/acs.jmedchem.0c01435
J. Med. Chem. XXXX, XXX, XXX−XXX